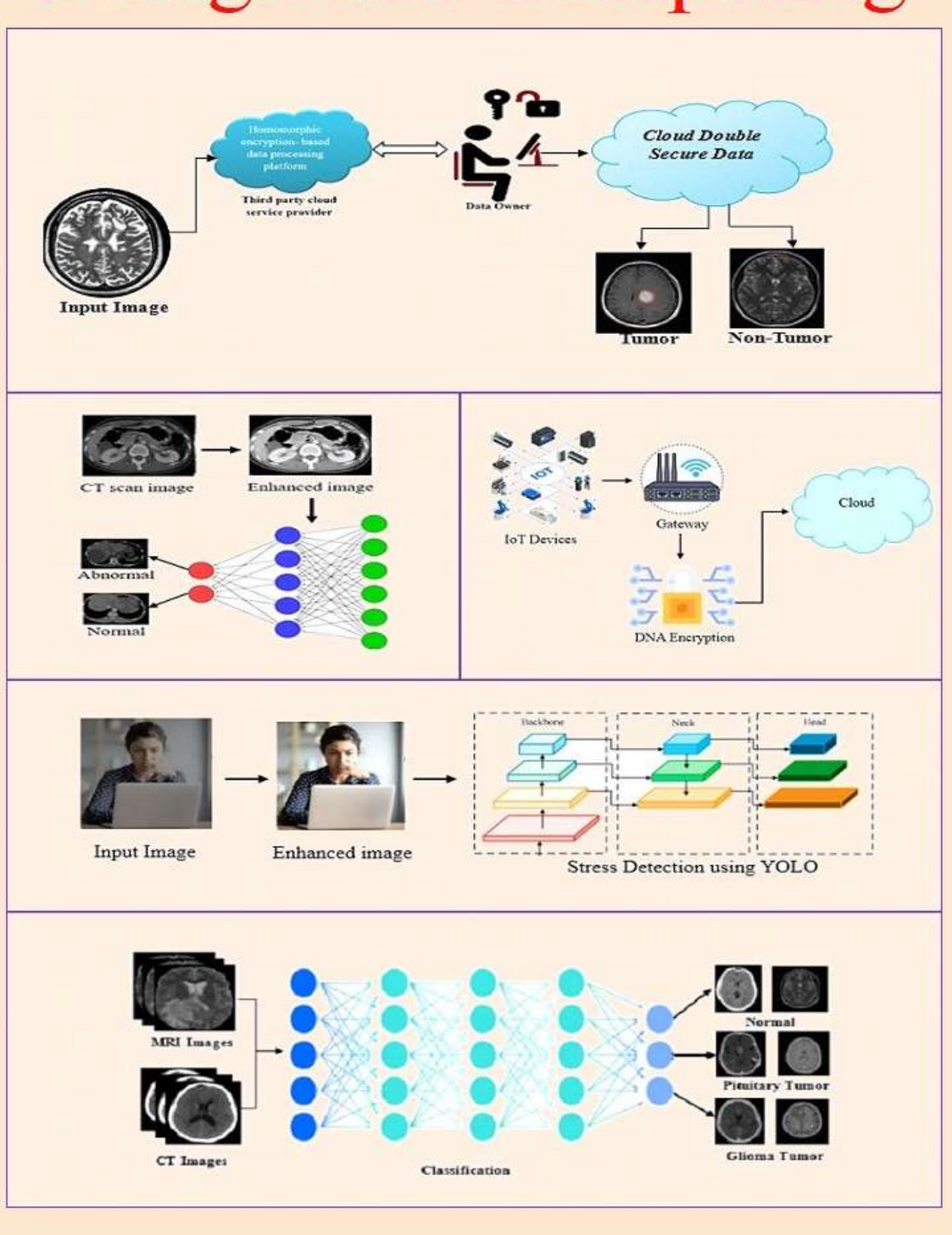


IJSDC

ISSN: XXXX - XXXX

International Journal of System Design and Computing

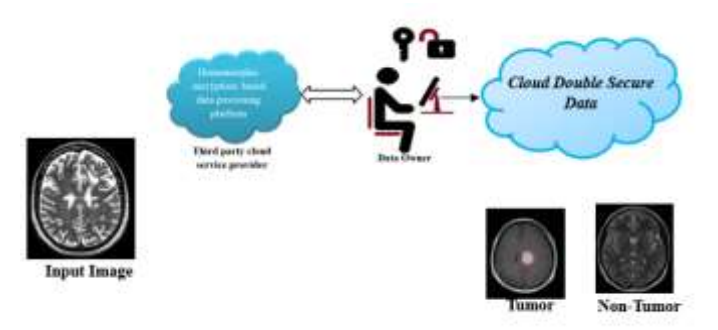


International Journal of System Design and Computing

1. DOUBLE SECURE CLOUD MEDICAL DATA USING EUCLIDEAN DISTANCE-BASED OKAMOTO UCHIYAMA HOMOMORPHIC ENCRYPTION

M. Anisha and V. Adlin Beenu

Abstract – Electronic Medical Records (EMRs) are computerized copies of paper records used in healthcare settings. Data from these systems allows doctors to quickly access and manage patients' medical records at healthcare institutions. Medical data security safeguards patients' rights and the duties of healthcare workers. Sharing such medical records with another medical organization is challenging for them. Cloud computing (CC) is the most effective way for storing this sort of data and addressing these issues. In this research a novel DOuble SEcure MEDical Cloud data (DOSE MED) technique has been proposed that enhances privacy and security of medical data. The proposed DOSE MED



method consists of three stages namely, registration phase, encryption phase and storage/decision phase. The proposed method utilizes Okamoto Uchiyama's homomorphic encryption technique to add prediction capability on the cloud which paves the way for disease prediction by medical practitioners. Euclidean distance-based classifier has been used for predicting data without decrypting it. The security findings demonstrate that the proposed DOSE MED provides selective security for the chosen keyword assaults. Performance analysis and real-world simulation trials demonstrate that this system is both efficient and practicable.

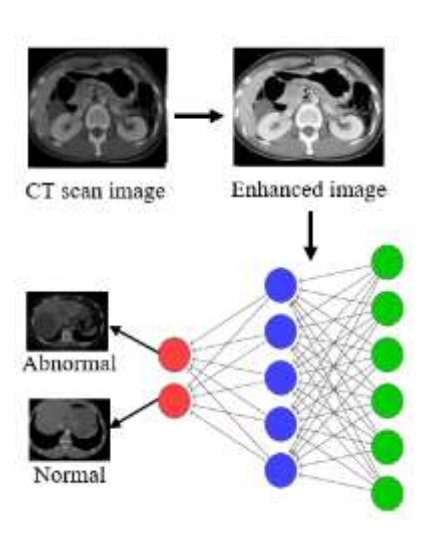
Keywords - Okamoto Uchiyama homomorphic encryption, Electronic Medical Records, Cloud computing.

2. GASTRIC CANCER DETECTION VIA DEEP LEARNING IN IMAGE PROCESSING

R. Tharani and C. Jasphin

Abstract – Gastric cancer (GC) is one of the leading causes of mortality from cancer around the world. It primarily affects older persons. Every year, almost six out of ten persons diagnosed with stomach cancer are above the age of 65. This paper proposed a novel GAstric cancer Detection using DEep LEarning (GADDLE) to identify the gastric cancer in an CT image. Initially the input images are pre-processed using the Gaussian adaptive bilateral filter to enhance the quality of the image. Therefore, the pre-processed images are fed into RegNet feature extraction model to for extracting the features in the image. The best features are selected by using the Dingo Optimization Algorithm. Finally, the normal and the abnormal case of the GC are classified using Link Net model. The GasHisSDB datasets are used to evaluate the performance of the proposed method of specific matrices such as Specificity, Recall, Accuracy, Precision and F1-Score. The suggested Link Net improves accuracy by 2.43%, 4.89%, and 1.98% compared to Alex Net, Google Net, and ResNet, respectively.

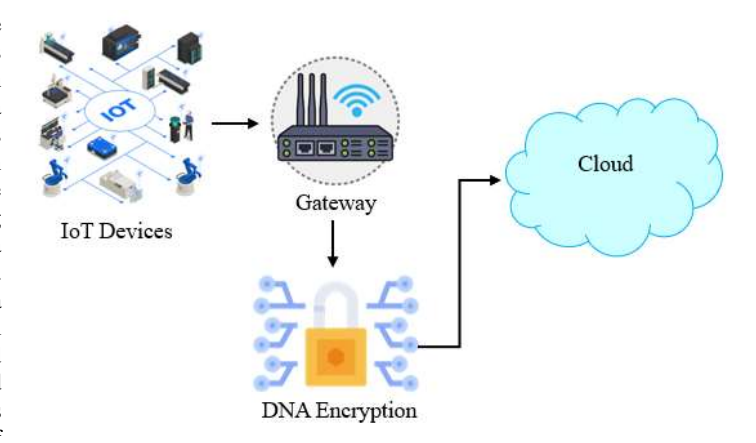
Keywords - Gastric cancer, Link Net, Dingo Optimization, Reg Net.



3. DNA ENCRYPTION-BASED SECURE ACCESS CONTROL AND DATA SHARING IN AN ENABLED CLOUD ENVIRONMENT

A.R. Aarthy and K. Vinoth Kanth

Abstract - IoT and cloud service providers are vulnerable to both internal and external threats consequently it is not possible to fully trust them with sensitive customer data. The cloud should offer a mechanism for the user to verify if the integrity of his data is being maintained or if it has been compromised, as the user cannot physically judge the data. Cloud computing is the best solution for storing this type of data. IoT has introduced secure data sharing and access management to prevent this issue. However, centralized access control presents a number of difficulties. The goal is to develop a novel DNA Encryption-based Secure Access Control and Sharing (DESACS) technique that has been proposed in an IoT-enabled Cloud environment which enhances the privacy and security of IoT data. The privacy of



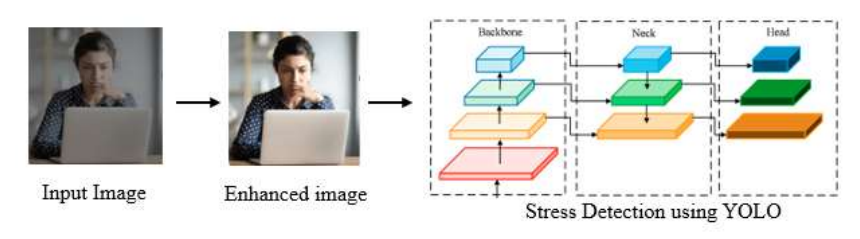
IoT has been increased by encrypting the data using the DNA cryptography (DNAC) encryption technique. It offers fresh hope for breaking invincible algorithms. This is a result of DNA computing's increased speed, low storage needs, and power consumption. In contrast to traditional storage media, which require 1012 nm3/bit, DNA stores memory at a density of roughly 1 bit/nm3.

Keywords - Internet of Things, DNA, Cloud, DNA Encryption

4. IT EMPLOYEES STRESS DETECTION BASED ON YOLO DEEP LEARNING ALGORITHM

S. Abinisha and S. S. Pooja

Abstract – Stress related disorders are extremely prevalent among workers in the corporate sector. The high demands and extended work hours of IT employment have led to an increase in stress among IT workers. In this paper a novel STress DEtection on it employees using YOLO deep learning (STEP-YOLO) has been proposed for



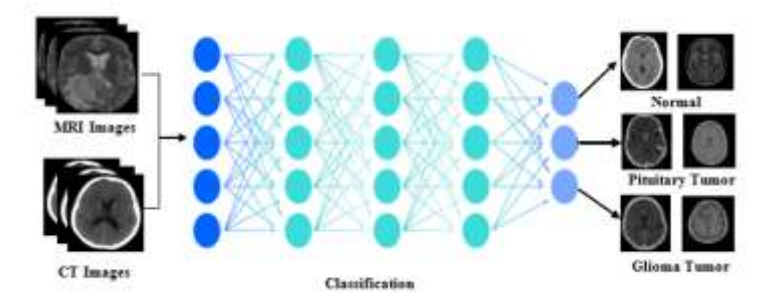
detecting the Stress on IT Employees. Initially, the input images are pre-processed in this pre-processing image acquisition and image processing are done to enhance the image. The features are extracted from the pre-processed image it extracts the feature whether they are happy, sad or neutral. Finally, the objects are detected using the YOLOv5 technique to detect the stress on IT employees. The proposed STEP-YOLO achieves an accuracy rate of 99.35% and an overall accuracy rate of 0.94%, 1.61% and 0.7% which is comparatively higher than the existing methods such as UBFC-Phys, PSS and SAD. The proposed method takes 0.18 milliseconds to detect the stress on IT employees which is comparatively less than the existing methods respectively.

Keywords - YOLOv5, Deep Learning, Stress Detection, IT Employees.

5. DEEP LEARNING MODEL FOR ACCURATE BRAIN TUMOR DETECTION USING CT AND MRI IMAGING

R. Abirami and P. Krishna Kumar

Abstract – Brain tumors (BT) are a very common, deadly condition with a very poor prognosis at the most aggressive grade. BT represent a prevalent and fatal condition with particularly poor prognosis at advanced stages. Accurate diagnosis and classification are critical for effective treatment planning and patient care. This study introduces a novel deep learning-based algorithm for early BT detection using CT and MRI images. The proposed model enhances image quality using Adaptive Trilateral filtering, extracts feature via the MobileNet model, selects relevant features through



the Tyrannosaurus optimization algorithm, and classifies brain tumors with a Deep Belief Network (DBN). The model categorizes tumors into three classes: pituitary tumor, no tumor, and glioma tumor. In comparison to conventional deep learning networks, the model performs better in experiments using the BRATS2020 dataset, reaching a 99.3% accuracy rate and great dependability. This paper offers significant improvements in automated brain tumor detection, promising better patient outcomes through early and precise diagnosis.

Keywords - Brain Tumor, Deep Learning, Deep Belief Network, Mobile Net.



RESEARCH ARTICLE

DOUBLE SECURE CLOUD MEDICAL DATA USING EUCLIDEAN DISTANCE-BASED OKAMOTO UCHIYAMA HOMOMORPHIC ENCRYPTION

M. Anisha^{1,*} and V. Adlin Beenu ²

*Corresponding e-mail: aninisha519@gmail.com

Abstract - Electronic Medical Records (EMRs) are computerized copies of paper records used in healthcare settings. Data from these systems allows doctors to quickly access and manage patients' medical records at healthcare institutions. Medical data security safeguards patients' rights and the duties of healthcare workers. Sharing such medical records with another medical organization is challenging for them. Cloud computing (CC) is the most effective way for storing this sort of data and addressing these issues. In this research a novel DOuble SEcure MEDical Cloud data (DOSE MED) technique has been proposed that enhances privacy and security of medical data. The proposed DOSE MED method consists of three stages namely, registration phase, encryption phase and storage/decision phase. The proposed method utilizes Okamoto Uchiyama's homomorphic encryption technique to add prediction capability on the cloud which paves the way for disease prediction by medical practitioners. Euclidean distancebased classifier has been used for predicting data without decrypting it. The security findings demonstrate that the proposed DOSE MED provides selective security for the chosen keyword assaults. Performance analysis and real-world simulation trials demonstrate that this system is both efficient and practicable.

Keywords – Okamoto Uchiyama homomorphic encryption, Electronic Medical Records, Cloud computing.

1. INTRODUCTION

ISSN: xxxx-xxxx

"Cloud computing" refers to the supply of numerous internet services such as networking, processing power, and storage [1]. This approach improves scalability, flexibility, and cost-efficiency by enabling users to access and store data and programs on remote servers rather than local hardware [2]. The main cloud service providers are Google Cloud Platform, Microsoft Azure, and Amazon Web Services (AWS). CC supports diverse applications from web hosting to big data analytics and machine learning [3,4].

Cloud computing in Electronic Medical Records (EMRs) enhances the storage, accessibility, and security of patient data [5]. It allows healthcare providers to access and update patient records in real-time from any location, improving collaboration and patient care. Cloud-based EMRs also offer scalable storage solutions and robust etc. [6]. Additionally, they enable compliance with regulations through advanced security measures and encryption. This technology supports telemedicine, facilitating remote consultations and continuous patient monitoring [7].

Security of medical data is crucial to protect sensitive patient data from breaches and unauthorized access [8]. This includes robust encryption, safe access restrictions, and frequent audits to assure data integrity and confidentiality. Compliance with standards such as HIPAA (Health Insurance Portability and Accountability Act) is critical, which requires special precautions for EHRs [9,10]. Additionally, educating healthcare staff on best security practices and using advanced threat detection systems can mitigate risks and enhance overall data security. The major contribution of the work has been followed by

- The proposed DOSE MED method consists of three stages namely, registration phase, Encryption phase, and storage/decision phase.
- In the registration phase, the patient and medical centre must have to register their identity with the network administrator to receive the medical EHR.
- In the Encryption phase, the medical centre generates an encrypted medical data by using DNA combined with Okamoto Uchiyama and stores in cloud storage.
- In the Storage/decision phase the encrypted medical health records from Medical Centre, will be

¹ Department of Computer Science and Engineering from Satyam College of Engineering and Technology, Aralvaimozhi, Anna University, India.

² Department of Computer Science and Engineering, Arunachala college of Engineering for Women, Manavilai, Anna University Chennai, India.

computed without being decrypted and takes decision about prediction based on Euclidean distance classifier.

The remaining portion of the work has been followed by, section 2 represents the literature review of the proposed, section 3 represents the proposed methodology, section 4 represents the introduction of the proposed, and section 5 represents the conclusion and future work of the proposed methodology.

2. LITERATURE SURVEY

The objective of the literature survey is to provide a concise overview as well as full information regarding current systems. The purpose of the literature survey is to thoroughly define the technical specifics associated with the primary project in a brief and straightforward way.

In 2023 Boomija, M.D. and Raja, S.K., [11] developed the Secure Partially Homomorphic Encryption (SPHE) algorithm to encrypt the data that is outsourced and to operate on the ciphertext by multiplying and dividing it. This technique is especially useful for computing on data that is outsourced and protecting patient electronic health records.

In 2023 Rahmani, P., et al., [12] developed a revolutionary technique for relational databases that combines data concealing and secret sharing to safeguard the confidentiality and secrecy of secret characteristics. One or more cover characteristics in a relation are embedded into one or more hidden attributes in the same relation. A set of shares columns is designed to seem to be connected with just the cover attributes.

In 2022 Pan, H., et al., [13] suggested an IoT medical data sharing program with cloud-chain collaboration and policy fusion. A dispute resolution and fusion technique that permits co-authorization of medical data by the patient and the physician is introduced in relation to asymmetric access control rights. Experiments proved that the suggested

technique is feasible, and the security analysis indicated that it meets the requirements of secrecy and verifiability of the recovered information.

In 2022 Kartit, A., [14] proposed a new strategy for maintaining data secrecy, based on Hadoop MapReduce operations and a multi-agent system. Furthermore, to build intelligent distributed computing for effective management of Virtual Machine (VM) workloads, a method based on the Bat Algorithm (BA) was adopted.

In 2023 Alabdulatif, A., et al., [15] proposed a new cloud-based hybrid access control system for securing medical big data in healthcare enterprises. The study's findings indicate that the access control approach can resist the majority of assaults and serve as the cornerstone for further secure and safe medical big data solutions.

In 2022 Ramachandra, M.N., et al., [16] developed the use of the Triple Data Encryption Standard (TDES) approach to secure massive data in cloud environments. By making the Data Encryption Standard (DES) keys larger, the suggested TDES approach offers a comparatively easier solution to safeguard data privacy and prevent assaults. The outcomes of the trial demonstrated how well the suggested TDES approach secures and protects massive healthcare data on the cloud.

In 2022 Alluhaidan, A.S., [17] presented a unique method for guaranteeing storage and access safety using integrated transformed Paillier and KLEIN algorithms (ITPKLEIN-EHO), which leverages elephant herd optimizations (EHOs) to offer lightweight features. This proposed method's experiments on several EEG data sets for implementation are conducted using MATLAB.

3. PROPOSED METHODOLOGY

In this research a novel DOuble SEcure MEDical Cloud data (DOSE MED) technique has been proposed that enhances privacy and security of medical data.

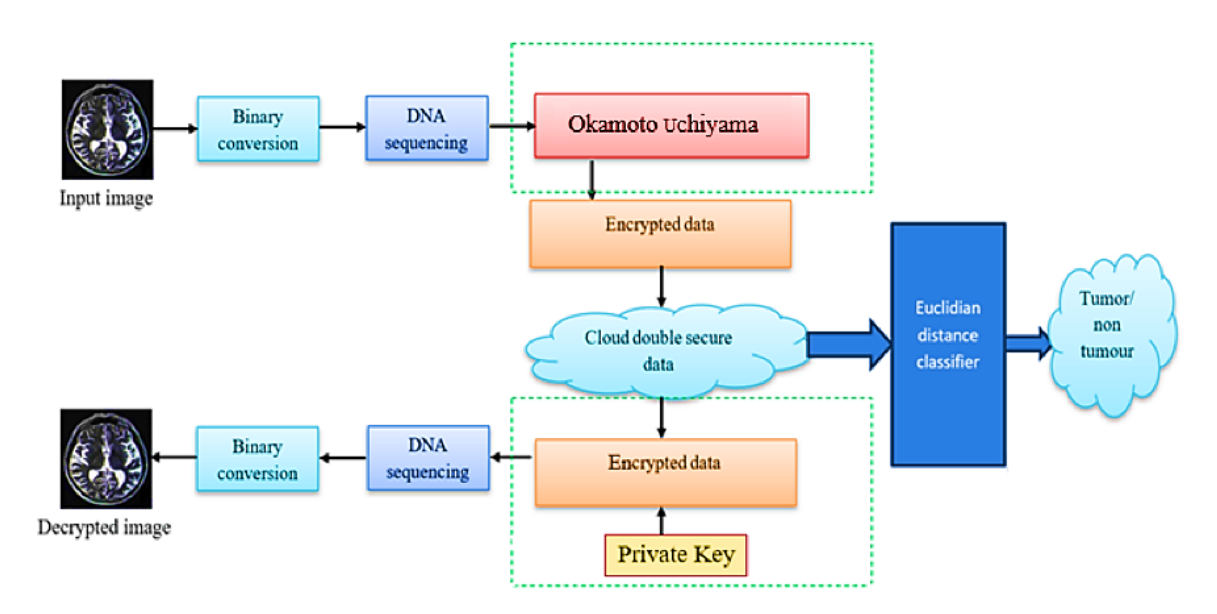


Figure 1. proposed methodology

The proposed DOSE MED method consists of three stages namely, registration phase, encryption phase and storage/decision phase. The proposed method utilizes Okamoto Uchiyama's homomorphic encryption technique to add prediction capability on the cloud which paves the way for disease prediction by medical practitioners. Euclidean distance-based classifier has been used for predicting data without decrypting it. The security findings demonstrate that the proposed DOSE MED provides selective security for the chosen keyword assaults.

The identity theft, will result in major financial troubles as well as a great deal of inconvenience in the life that can last for years. But it far worse in certain respects. If an identity thief tampers with the medical data, the file may contain inaccurate information about user's medical history and diagnosis. An OU algorithm is then used to encrypt the DNA sequences. After encryption, the encrypted image can be safely stored in the cloud. Using Euclidean distance classifier, the images can be compared for prediction.

The architecture of the proposed DOSE MED method is depicted in Figure 1. The suggested plan established a secure conduit for the provably safe storage of electronic medical records. To be more precise, the physician makes a diagnosis and creates a medical record after the patient registers on the hospital system. The medical facility must keep the records on file so that the patient may access his information at any time and the researcher can always find out specifics. Medical records must be encrypted before being saved as they include information pertaining to the patient's private. Here, the data are encrypted using DNA OU-HE server and then uploads it to the database for storage.

3.1. Binary Conversion

Binary conversion is the process of converting a number from the decimal (base-10) system to the binary (base-2) system. In binary, each digit represents a power of 2, starting from 2^0 on the right. For example, the decimal number 10 is converted to binary by determining the highest power of 2 less than or equal to 10, which is 8 (2^3). The next highest power of 2 is 2 (2^1), and then 0 (2^0). Therefore, 10 in decimal is represented as 1010 in binary. This method involves repeated division by 2 and recording the remainders.

3.2. DNA Sequencing Conversion

Deoxyribose Nucleic Acid is the abbreviation for DNA. DNA is a polymer made up of deoxyribonucleotides, which are monomers. Each nucleotide is made up of three fundamental components: deoxyribose sugar, phosphate group, and a nitrogenous base. Purines (Adenine and Guanine) and pyrimidines are the two forms of nitrogenous bases (Cytosine and Thymine). They are denoted by the letters A, G, C, and T. G connects to C, while A binds to T. The binary values for the DNA bases are displayed in Table 1. The order of bases may be ascertained by DNA sequencing, and in simple sequence format, they can be illustrated by a single letter.

Table 1. Binary values for DNA Bases

DNA	BINARY VALUES
A	00
G	01
C	10
T	11

DNA encryption is the technique of using a statistical approach to hide genetic information to increase genetic privacy in DNA sequencing operations. The goal is to figure out the approaches that are reliable and the role of legislation in assuring that the genetic privacy is protected indefinitely.

3.3. Okamoto Uchiyama [OU]

The OU cryptosystem was created in 1998 by Tatsuaki Okamoto and Shigenori Uchiyama. It is a public key cryptosystem. It makes use of $(\mathbb{Z}/n\mathbb{Z})$ *, the multiplicative group of integers modulo n. N applies the p2q evaluation, where p and q are big prime numbers.

3.3.1. OU Homomorphic Encryption [OU-HE]

HE is the procedure of encoding data into ciphertext that can be parsed and employed like the original ciphertext. OU Homomorphic encryption enables complex mathematical operations on encrypted data without needing decryption. OU claims that the OU cryptosystem satisfies the requirements for homomorphic encryption (HE) in this work. With HE, encrypted data may be computed without needing to be initially decrypted. Data owners that need to transmit data to the cloud for processing but do not trust the service provider with the unencrypted data frequently utilize HE. The data owner transmits the data to the server after encrypting it using a HE technique. Without first decrypting the data, the server then uses the encrypted data to carry out the required calculations and sends the encrypted results back to the data owner. Since the private key is unique to the data owner, only they are able to decipher the outcome. Figure 2 illustrates the example of the OU Homomorphic encryption.

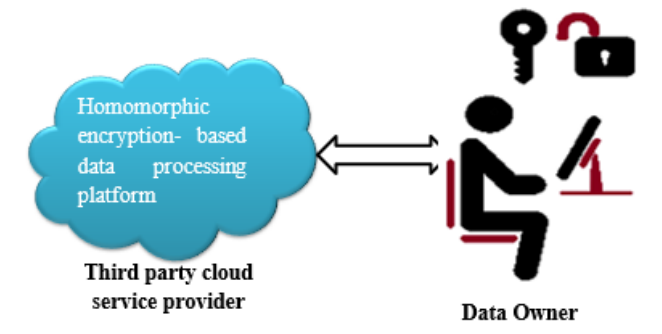


Figure 2. Homomorphic Encryption

3.3.2. OU Homomorphic Decryption

Decryption technology transforms encrypted code or data into a form that can be easily understood and read by humans or machines. This is basically called decrypting encrypted data. This happens on the receiving side. Messages can be decrypted using private or private keys. The diagram below clearly shows the decryption technique and the

ciphertext. H. The ciphertext is converted back to the original message.

3.4. Euclidean distance classifier

Euclidean distance is the most widely used point-todistance measurement. Based on this distance metric, the classifier is straightforward and easy to use. The Euclidean distance rule uses the mean class values as class centers to compute pixel-center distances. This technique is superior for classifying a monogenous area at the main level. Its quick classification time is what makes it advantageous. Euclidean distance can be used as a basic similarity measure to compare pixel values between an image under consideration and a reference image (e.g., a healthy image). If the Euclidean distance is significantly different from a threshold, it might indicate the presence of a disease or anomaly. Since Euclidean distance yields superior results than other techniques of distance estimation, it is employed. Since the method does not make judgments based on the original data, it is nonparametric. The following formula can be utilized to evaluate the Euclidean distance (Figure 3).

$$D = \sqrt{(A_1 - YB_1)^2 + (A_2 - B_2)^2 + \dots + (A_n - B_n)^2}$$

$$Y_2$$

$$Y_1$$

$$X_1$$

$$X_2$$

$$X_2$$

$$X_3$$

$$X_4$$

$$X_4$$

$$X_5$$

$$X_4$$

Figure 3. Calculation of Euclidean distance

Based on the difference in the pixel values the disease will be predicted by using the reference image that is encrypted and stored in the cloud.

4. RESULT AND DISCUSSION

The framework's assessment metrics specify the stakeholders, functions, and addressed problems to help meet privacy standards. This study's novel setup was developed using MATLAB 2019b, a deep learning toolkit.

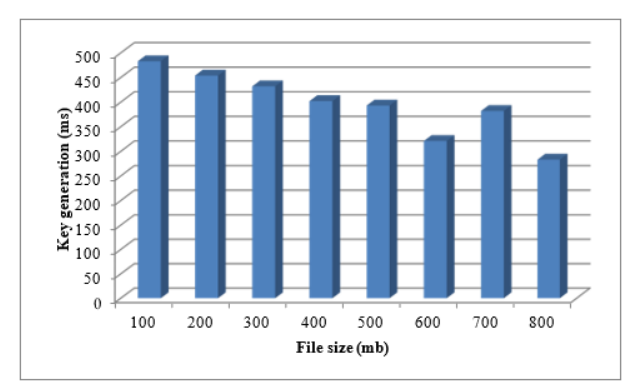


Figure 4. Performance analysis of key generation in DOSE MED

The graphical representation of the suggested technique for key generation is given in Figure 4. The recommended technique's key generation is compared to its file size. The file size of the suggested approach varies from 100 to 800 MB depending on the key generation. The recommended solution has a file size of 100 MB and generates keys in 487 milliseconds. The suggested technology generates keys in 323 milliseconds and has a file size of 600 megabytes. The key generation of the suggested methodology varies according on the file size of the proposed method.

Figure 5 depicts the suggested method's encryption time depending on encryption time. The proposed model encryption time is evaluated using data that can be encrypted with the encryption algorithm. The encryption time can be estimated using the proposed method's file size. The method's encryption time varies depending on the file size of the suggested method.

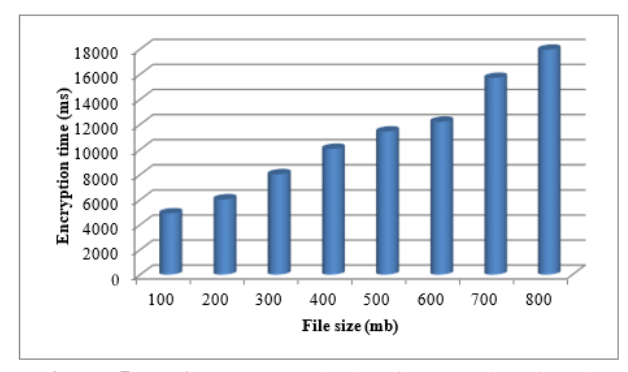


Figure 5. Performance analysis of encryption time in DOSE MED

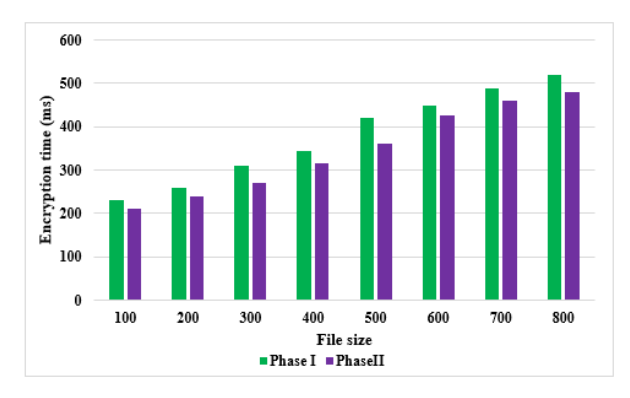


Figure 6. Encryption time comparison

A comparison of the proposed technique and the existing techniques is shown in Figure 6. The encryption time of the suggested DOSE MED technique is better than the existing method BACK method. This encryption time of the technique is based on the file size of the method which varies from 100 to 800 Mb. By comparing the proposed and the existing method, the proposed method is very much better than the existing method.

A comparison of the proposed technique and the existing techniques is shown in Figure 7. The encryption time of the suggested DOSE MED technique is better than the existing method BACK method. This encryption time of the technique is based on the file size of the method which varies from 100 to 800 Mb.

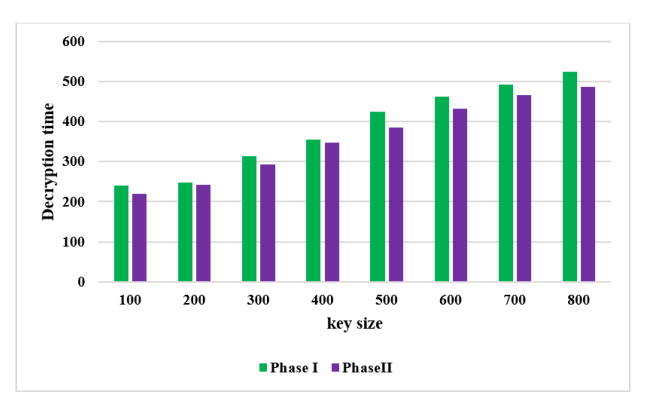


Figure 7. Decryption time comparison

5. CONCLUSION

In this paper a novel Double Secure medical Cloud data MED) using DNA Okamoto Uchiyama homomorphic encryption technique has been proposed in this work. Through the use of OU-HE technology, the method offers effective access control for electronic medical records, preventing unauthorized individuals from viewing the patient's confidential information. In addition, the Euclidean distance classifier aids in data prediction, data originality and traceability, and the resolution of central authority security deficiencies. All of these factors were taken into consideration while utilizing the cloud storage platform to guarantee the safe storage of medical data. However, this scheme still has some shortcomings, such as the access privilege and require specialized storage infrastructure and may lead to increased storage costs, then the Error Rates of the data stored. The proposed secure data transmission scheme will be extended to work in an uncontrolled environment in future by focusing on enhancing the efficiency and security of DNA-based OU-HE methods. This includes developing more robust encryption algorithms that can handle larger medical images and reduce computation overhead.

CONFLICTS OF INTEREST

The authors declare that they have no known competing financial interests or personal relationships that could have appeared to influence the work reported in this paper.

FUNDING STATEMENT

Not applicable.

ACKNOWLEDGEMENTS

The author would like to express his heartfelt gratitude to the supervisor for his guidance and unwavering support during this research for his guidance and support.

REFERENCES

- [1] G.R. Babu, P.V. Chintalapati, P.K. Sree, A. Pudi, and C.V. Ramana, "A Context Sensitive with Effective Task Migration in Mobile Cloud Computing Services", *In 2023 3rd International Conference on Computing and Information Technology (ICCIT)*, pp. 201-205, 2023. IEEE. [CrossRef] [Google Scholar] [Publisher Link]
- [2] Y.C. Wang, J. Xue, C. Wei, and C.C.J. Kuo, "An overview on generative ai at scale with edge-cloud computing", *IEEE Open*

- Journal of the Communications Society, 2023. [CrossRef] [Google Scholar] [Publisher Link]
- [3] R.R. Irshad, S. Hussain, I. Hussain, J.A. Nasir, A. Zeb, K.M. Alalayah, A.A. Alattab, A. Yousif, and I.M. Alwayle, "IoT-Enabled Secure and Scalable Cloud Architecture for Multi-User Systems: A Hybrid Post-Quantum Cryptographic and Blockchain based Approach Towards a Trustworthy Cloud Computing", IEEE Access. 2023. [CrossRef] [Google Scholar] [Publisher Link]
- [4] S.S. Vellela, B.V. Reddy, K.K. Chaitanya, and M.V. Rao, "An integrated approach to improve e-healthcare system using dynamic cloud computing platform", *In 2023 5th International Conference on Smart Systems and Inventive Technology (ICSSIT)*, pp. 776-782, 2023. IEEE. [CrossRef] [Google Scholar] [Publisher Link]
- [5] H.B. Mahajan, A.S. Rashid, A.A. Junnarkar, N. Uke, S.D. Deshpande, P.R. Futane, A. Alkhayyat, and B. Alhayani, "RETRACTED ARTICLE: Integration of Healthcare 4.0 and blockchain into secure cloud-based electronic health records systems", *Applied Nanoscience*, vol. 13, no. 3, pp. 2329-2342, 2023. [CrossRef] [Google Scholar] [Publisher Link]
- [6] V. Chamola, A. Goyal, P. Sharma, V. Hassija, H.T.T. Binh, and V. Saxena, "Artificial intelligence-assisted blockchain-based framework for smart and secure EMR management", Neural Computing and Applications, vol. 35, no. 31, pp.22959-22969, 2023. [CrossRef] [Google Scholar] [Publisher Link]
- [7] G. Peng, A. Zhang, and X. Lin, "Patient-centric fine-grained access control for electronic medical record sharing with security via dual-blockchain", *IEEE Transactions on Network Science and Engineering*, 2023. [CrossRef] [Google Scholar] [Publisher Link]
- [8] S. Bera, S. Prasad, and Y.S. Rao, "Verifiable and Boolean keyword searchable attribute-based signcryption for electronic medical record storage and retrieval in cloud computing environment", *The Journal of Supercomputing*, vol. 79, no. 18, pp.20324-20382, 2023. [CrossRef] [Google Scholar] [Publisher Link]
- [9] S. Fugkeaw, L. Wirz, and L. Hak, "Secure and Lightweight Blockchain-enabled Access Control for Fog-Assisted IoT Cloud based Electronic Medical Records Sharing", IEEE Access, 2023. [CrossRef] [Google Scholar] [Publisher Link]
- [10] R. Akangbe, and T. Charles-Chinkata, "Dealing with Data Breaches on Patient's EMR Sensitive Data: A Comprehensive Approach," Frontiers in Digital Health, 2024. [CrossRef] [Google Scholar] [Publisher Link]
- [11] M.D. Boomija, and S.K. Raja, "Securing medical data by role-based user policy with partially homomorphic encryption in AWS cloud", *Soft Computing*, vol. 27, no. 1, 559-568, 2023. [CrossRef] [Google Scholar] [Publisher Link]
- [12] P. Rahmani, M. Taheri, and S.M. Fakhrahmad, "A novel secure data outsourcing scheme based on data hiding and secret sharing for relational databases", *IET Communications*, vol. 17, no. 7, pp. 775-789, 2023. [CrossRef] [Google Scholar] [Publisher Link]
- [13] H. Pan, Y. Zhang, X. Si, Z. Yao, and L. Zhao, "MDS 2-C 3 PF: A Medical Data Sharing Scheme with Cloud-Chain Cooperation and Policy Fusion in IoT", Symmetry, vol. 14, no. 12, pp. 2479, 2022. [CrossRef] [Google Scholar] [Publisher Link]

- [14] A. Kartit, "New Approach Based on Homomorphic Encryption to Secure Medical Images in Cloud Computing," *Trends in Sciences*, vol. 19, no. 9, pp. 3970-3970, 2022. [CrossRef] [Google Scholar] [Publisher Link]
- [15] A. Alabdulatif, N.N. Thilakarathne, and K. Kalinaki, "A Novel Cloud Enabled Access Control Model for Preserving the Security and Privacy of Medical Big Data", *Electronics*, vol. 12, no. 12, pp.2646, 2023. [CrossRef] [Google Scholar] [Publisher Link]
- [16] M.N. Ramachandra, M. Srinivasa Rao, W.C. Lai, B.D. Parameshachari, J. Ananda Babu, and K.L. Hemalatha, "An efficient and secure big data storage in cloud environment by using triple data encryption standard", *Big Data and Cognitive Computing*, vol. 6, no. 4, pp.101, 2022. [CrossRef] [Google Scholar] [Publisher Link]
- [17] A.S. Alluhaidan, "Secure Medical Data Model Using Integrated Transformed Paillier and KLEIN Algorithm Encryption Technique with Elephant Herd Optimization for Healthcare Applications", *Journal of Healthcare Engineering*, 2022. [CrossRef] [Google Scholar] [Publisher Link]

AUTHORS



M. Anisha she was born in Kanyakumari district, Tamilnadu, India in 2000. She received her BE degree in Computer Science and Engineering from Arunachala college of Engineering for Women, Manavilai, Anna University, currently she is pursuing her ME degree in Computer Science and Engineering from Satyam College of Engineering and Technology, Aralvaimozhi, Anna University, India. Her interested research area is cloud computing, and Internet of Things, Image Processing.



V. Adlin Beenu She received her BE degree in computer science and engineering from Arunachala college of engineering for women, Manavilai, Anna University. She received her ME degree in computer science and engineering from Arunachala college of engineering for women, Manavilai, Anna University Chennai. Her interested research area is IOT, Data science, and image processing.

Arrived: 06.05.2024 Accepted: 02.06.2024



RESEARCH ARTICLE

GASTRIC CANCER DETECTION VIA DEEP LEARNING IN IMAGE PROCESSING

R. Tharani 1,* and C. Jasphin 2

¹ Department of Computer Science Engineering, Arunachal College of Engineering for Women, Manavilai, Nagercoil, Tamil Nadu 629203 India.

² Department of Computer Science and Engineering, Manavilai, Nagercoil, Tamil Nadu, Anna University, Chennai, India.

*Corresponding e-mail: tharaniram2018@gmail.com

Abstract - Gastric cancer (GC) is one of the leading causes of mortality from cancer around the world. It primarily affects older persons. Every year, almost six out of ten persons diagnosed with stomach cancer are above the age of 65. This paper proposed a novel GAstric cancer Detection using DEep LEarning (GADDLE) to identify the gastric cancer in an CT image. Initially the input images are pre-processed using the Gaussian adaptive bilateral filter to enhance the quality of the image. Therefore, the pre-processed images are fed into RegNet feature extraction model to for extracting the features in the image. The best features are selected by using the Dingo Optimization Algorithm. Finally, the normal and the abnormal case of the GC are classified using Link Net model. The GasHisSDB datasets are used to evaluate the performance of the proposed method of specific matrices such as Specificity, Recall, Accuracy, Precision and F1-Score. The suggested Link Net improves accuracy by 2.43%, 4.89%, and 1.98% compared to Alex Net, Google Net, and ResNet, respectively.

Keywords - Gastric cancer, Link Net, Dingo Optimization, Reg Net.

1. INTRODUCTION

ISSN: xxxx-xxxx

Gastric cancer is the fifth most common cancer worldwide and the third greatest cause of cancer-related death [1]. Every year, more than a million new instances of stomach cancer are reported worldwide, making it a major public health concern. GC is still the third most prevalent cause of cancer-related death globally, despite a reduction in incidence and mortality over the last 50 years [2]. There are numerous immutable risk factors for stomach cancer, including age, sex, and race/ethnicity. Some risk factors, like smoking, eating a diet high in nitrates and nitrites, and having Helicobacter pylori infection, are under your control [3]. The survival percentage of patients with stomach cancer varies significantly based on their diagnosis date. Early detection of stomach cancer can lead to a survival rate of more than 90% [4]. GC incidence varies widely, with higher frequencies in Asia, Africa, South America, and Eastern Europe. In Western countries, the number of patients in the proximal stomach appears to be growing, despite a consistent drop in absolute incidence over recent decades [5].

In recent years, with the introduction of deep learning, artificial intelligence (AI) has increasingly been used in medical image processing and has displayed excellent performance in recognizing lesions under upper or smaller endoscopy of the stomach in different modes, such as WLE, ME-NBI, or blue laser imaging [6]. A deep learning technique identified stomach cancer with a sensitivity of nearly 100% and a specificity of 80.6% in 3212 real-world WSIs scanned by multiple scanners. In an internal test, the algorithm fared comparable to 12 pathologists in terms of assessment [7]. The Efforts are being made to improve imaging technologies and develop models for predicting the lymph nodal status of patients with early gastric cancer, but the diagnostic accuracy of endoscopic ultrasonography (EUS) and enhanced computed tomography (CT) for LNM prediction remains unsatisfactory [8]. Personalized therapy strategies for stomach cancer rely on accurate outcome prediction [9]. Therefore, novel technique has been proposed to gastric cancer in an CT image. The suggested work's main contribution is as follows.

- Initially, the input photos are pre-processed with a Gaussian adaptive bilateral filter to improve their quality.
- Therefore, the pre-processed images are fed into the Reg Net model for extracting the features in the image.
- Afterward the best features are selected from the extracted features utilizing Dingo Optimization algorithm.
- Finally, the normal and abnormal cases of the GC is classified employing Link Net model.

The rest of this study's sections are explained below: Section II reviews the research in light of existing literature. Section III provides a comprehensive description about the proposed system. The conclusion is found in Section V, whilst the results and discussion are in Section IV.

2. LITERATURE SURVEY

The detection of gastric cancer forms using deep learning techniques has been part of numerous studies in recent years. A quick summary of a few current research papers is given in the section as follows.

In 2020, Li, L., et al [10] suggested a method for analysing stomach mucosal lesions detected by M-N [BI that is based on convolutional neural networks (CNNs). The Microvascular architecture and the micro surface structure of gastric mucosal lesions are observed using Magnifying Endoscopy with Narrow Band Imaging (M-NBI), which has been used to investigate early stomach cancer. The CNN system's sensitivity, specificity, and accuracy for early diagnosis of gastric cancer were 91.18%, 90.64%, and 90.91%, respectively.

In 2020, Horiuchi, Y., et al [11] suggested a technique towards the early identification of gastric cancer (EGC), This allows the adoption of less intrusive cancer treatments. The primary goal is to investigate the extent to which the CNN system can diagnose gastritis and EGC using ME-NBI. The CNN accurately classified 220 out of 258 ME-NBI images, demonstrate the accuracy rate of 85.3%. In the future, the CNN system and endoscopists will be able to diagnose cases by confirming by biopsy whether the lesions are due to gastritis or gastric cancer.

In 2021, Wang, J. and Liu, X., [12] proposed a Deeplab v3+ neural network-based automatic model for gastric cancer segmentation. It evaluates the sensitivity, specificity, accuracy, and dice coefficient of a multi-scale input Deeplab v3+ network to SegNet and ICNet. Similar to the SegNet and Faster-RCNN models, Deeplab v3+ has an accuracy of 95.76% and a Dice coefficient of 91.66%, which is more than 12% higher. Future research should concentrate on evaluating and enhancing techniques to produce DL models for cancer diagnosis that perform better.

In 2022, Chen, H., et al [13] proposed a multi-scale visual transformer model for gastric histopathological image detection known as GasHisTransformer (GHID). The suggested approach will enable automatic worldwide detection of stomach cancer photos. With accuracy rates of 96.43% and 97.97%, GasHisTransformer and LW-GasHisComponents are tested using a dataset of stomach cancer histology. The techniques like few-shot learning and domain adaptation to address this issue in further research.

In 2021, Lee, S.A., et al [14] proposed a CADx method to diagnose and categorize cancerous diseases such gastric polyps, gastric ulcers, gastritis, and bleeding from cases of gastric cancer. In order to choose efficient treatment alternatives without requiring a surgical biopsy, this process may be quite important. In classifying cancer and non-cancer cases, this method achieved 96.3% accuracy. In the future, this study's findings will be confirmed by using the CADx system on a bigger, independent data set.

In 2022, Su, F., et al [15] suggested a deep learning (DL) system that uses hematoxylin-eosin (HE) to directly detect microsatellite instability (MSI) and interpretable tumor differentiation grade in gastric cancer. This method will

gather pathological information regarding the formation of glandular structures, which is essential for differentiating between PDA and WDA. Applying the best tile fusion classifier, the integrated system achieved automatic patient-level MSI diagnosis with an accuracy of 83.87%.

In 2022, Wu, L., et al [16] proposed a system using deep learning to address numerous aspects of early gastric cancer diagnosis, including as recognizing and forecasting cancer and detecting stomach neoplasms. For a national human-machine competitors, this technique provides a cutting-edge comparison of the system to endoscopists via real-time films. The predictive system's accuracy ratings for early gastric cancer invasion depth and differentiation status were 71.43% and 78.57% respectively.

The literature review indicates that a number of techniques focus on CT input image to accurately diagnosis the gastric cancer in the early stage. Although as previously mentioned there are certain disadvantages to these approaches. To overcome this drawback a novel GAstric cancer Detection using DEep LEarning (GADDLE) have been proposed to identify GC in CT images.

3. PROPOSED METHOD

This paper proposed a novel GAstric cancer Detection using DEep LEarning (GADDLE) to identify the gastric cancer in an CT image. Initially the input images are preprocessed using the Gaussian adaptive bilateral filter to enhance the quality of the image. Therefore, the preprocessed images are fed into RegNet feature extraction model to for extracting the features in the image. The best features are selected by using the Dingo Optimization Algorithm. Finally, the normal and the abnormal case of the GC are classified using Link Net model (Figure 1).

3.1. Gaussian Adaptive Bilateral filter

The Gaussian Adaptive Bilateral (GAB) Filter is a bidirectional filtering extension that adjusts its filtering coefficients based on local image data, creating a dependable tool for image denoising with edge-preserving smoothing. This filter reduces noise in photos entered during the preprocessing step. The GAB filter effectively reduces noise from images while enhancing edge preservation and smoothness.

The technology suggested has the ability to greatly improve image quality. The bilateral filter, input image I_l , and guiding G are distinct, as illustrated in equation (1):

$$P(c) = \sum_{r} (w_{cr}^{\hat{G}}) (\hat{G}) I_{l} \tag{1}$$

Equation (1) defines I_l as the center point of the input picture, while equation (2) expresses $w_{c,r}^{G_1}$.

$$W_{c,r}^{G_1} = \frac{1}{M_c} \exp\left[-\left|\frac{c-r}{-\rho_e^2}\right|\right|^2\right]$$
 (2)

In equation (2), M_c represents the normalizing value, and the Gaussian spatial kernel is represented by exp $[-|\frac{c-r}{-\rho_e^2}|^2]$. The GAB kernel evaluation factor is expressed in the following equation.

(3)

Figure 1. Work flow of proposed (GADDLE) block diagram

3.2. RegNet

Statistical features such as average, median, variation, normalized entropy, standard deviation, and kurtosis are extracted from photos using RegNet during the feature extraction process. The graphical function is based on the lightweight and efficient RegNet foundation. RegNet proceeds in four steps with ever less pixels, employing a succession of comparable units. The subsequent section A^n represents the module output, A^{n-1} represents the feature map for the nth module. The pooling method is frequently used in featured systems to reduce the overall amount of feature representations by performing the required analysis. Stride (s=1) was employed to achieve maximum pooling. The framework's maximum input size is 224x224, which is the standard dimension of data for RegNet networks.

 $w_{c,r}^{q,f,u}(I_l, \hat{G}) = \frac{1}{M_c} \exp\left[-\left|\frac{c-r}{-\rho_c^2}\right|^2\right] \exp\left[-\left|\frac{I_1-\hat{G}}{-\rho_c^2}\right|^2\right]$

$$P_2^n = ReLU(q_m(w_{12}^n * Y_1^n + b_{12}^n)$$
(4)

$$[A^n,D^n] = ReLU(q_m\big(conLSTM(Z_2^P[A^{n-1},D^{n-1}])\big)) \qquad (5)$$

The input of ConLSTM inside the module is represented by the entry entity P_2^n and the previous output of ConvLSTM A^n in equation (5). The ConvLSTM determines whether the data inside the memory cell is supplied to the A^n output hidden characteristic map based on the inputs source.

3.3. Improved Dingo Optimization (IDO)

Improved Dingo Optimization's (IDO) optimization methodology is designed for feature selection, hence optimizing data and providing relevant features. Finding the most effective real-world system solutions is a difficult undertaking. Because there are plenty fantastic options

accessible. Equation (1) illustrates the improvement in persecution, scavenging, collective attack, and survival.

$$\delta = (AF - MF) \tag{6}$$

$$z = \frac{mean (Z(F-MF))}{mean (X(F-AF))}$$
 (7)

Here, $-\rho_e^2$ represents brightness fluctuations. Equations

(1) and (3) provide \hat{G} , and the range kernel is

$$DA = \delta \times \left(\frac{P}{Z}\right) \tag{8}$$

In this case, the terms AF and MF represent the best and worst objective functions, respectively. Fitness is represented by F, distance by A, generality by Y and p, and arbitrarily by DA, a value ranging from 0 to 1.

3.4. Link Net

The LinkNet architecture consists of a series of encoder and decoder units that break down and reconstruct the image, respectively. Finally, the images go through a few convolutional layers. The model was created with the goal of classifying cerebral palsy. LinkNet acts as a real-time semantic segmentation network. This keeps many of the image's spatial elements. The procedure comprises connecting the encoder module's shallow feature map to the similarly sized decoder module. This method uses the shallow layer's exact position data to decrease the need for superfluous computations and parameters, which speeds up computing without sacrificing precision.

In dilated convolutions, the dilated rate f_j represents subsampling the feature map by a factor of $f_j - 1$ or adding f_j zeros between the kernel weights. Equation (15) calculates

the size of the resulting f_j dilated convolution kernel for a 1*1 dilated kernel with size $a_i \times a_j$.

$$\hat{a}_i = a_i + (a_i - 1) \times (f_i - 1) = f_i \times (a_i - 1) + 1$$
 (9)

The LinkNet design differs greatly from neural networks in terms of pixel-wise operation. Its distinctiveness stems from the connection between the encoder and decoder. Spatial information is lost during decoding, and retrieving it from the encoder's output is difficult. LinkNet connects the

encoder and decoder using non-trainable pooling indices. This link recovers spatial information lost during encoding, which is critical for the decoder's up sampling. In this architecture, the decoder has fewer parameters and shares the knowledge gathered by the encoder. This design contributes to the creation of a more efficient network for real-time cerebral palsy classification when compared to existing architectural models. Link Net Architecture shown in Figure 2.

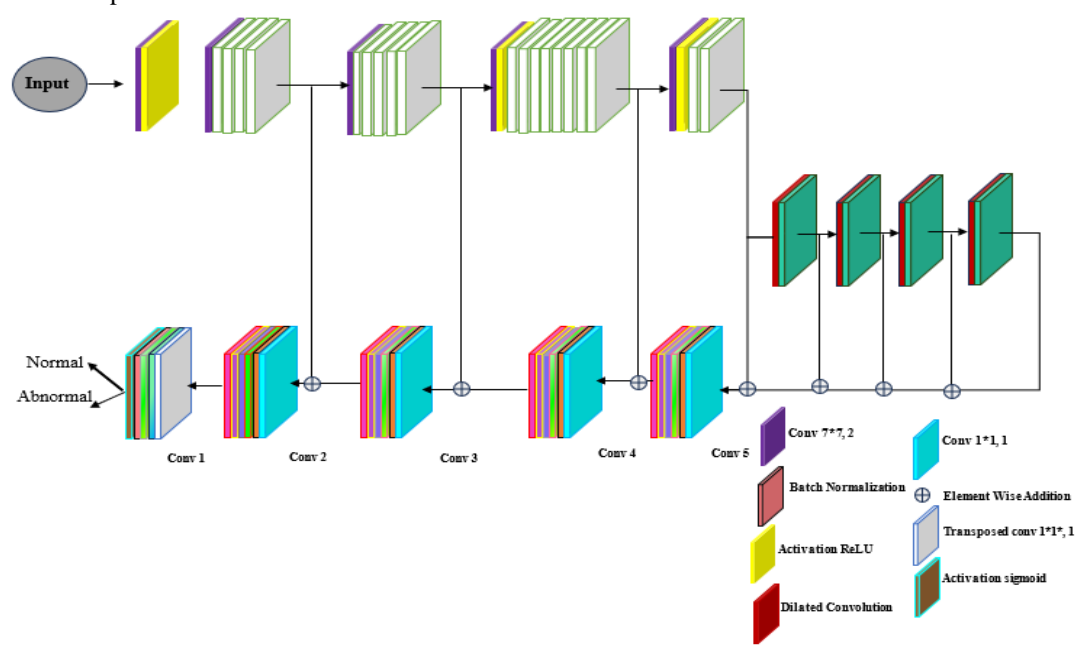


Figure 2. Link Net Architecture

4. RESULTS AND DISCUSSION

In the following section, the suggested model's efficiency is assessed using Matlab-2019b. The raw CT images are acquired from the GasHisSDB dataset [17], and they are pre-processed into appropriate frames for subsequent processing. The GasHisSDB dataset consists of 97,076 aberrant picture patches and 148,120 normal patches of images.

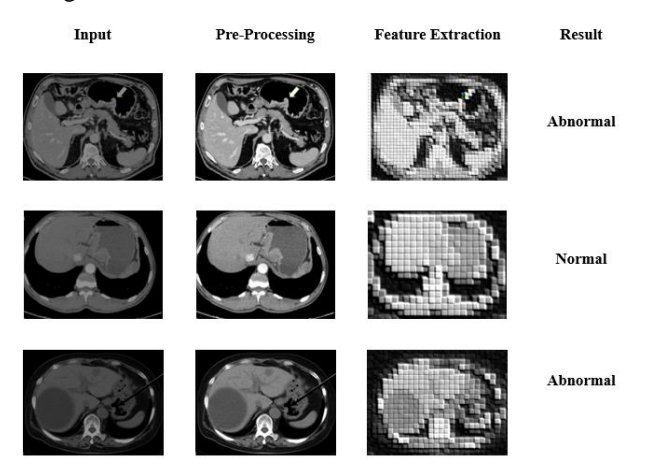


Figure 3. Experimental outcomes of the Proposed model

Figure 3 shows the visualization results of the suggested model using the acquired dataset. The input CT scans (column 1) are pre-processed with the GAB filter to remove

distortions and improve the quality of the input samples (column 2). At the same time, the pre-processed OCT pictures are fed into the RegNet model to extract the features (column:3) in images. Finally, DIO algorithm is used for feature selection and the Link Net model is utilized for the classification process to detect Normal, and abnormal cases (column:4).

4.1. Performance analysis

The abilities of the proposed model were assessed using particular metrics such as specificity, accuracy, recall, precision, and F1 score.

$$S = \frac{Neg_T}{Neg_T + PoS_F} \tag{10}$$

$$P = \frac{Pos_T}{Pos_T + Pos_T} \tag{11}$$

$$Recall = \frac{Pos_T}{Pos_T + Neg_F} \tag{12}$$

$$Accuracy = \frac{Pos_T + Neg_T}{Total\ no.of\ samples} \tag{13}$$

$$F1 \ score = 2 \left(\frac{Pre*Re}{Pre+Re} \right) \tag{14}$$

where Pos_T and Neg_T shows the genuine positives and negatives of the CT imagery. Pos_F and Neg_F indicates false positives and negatives in CT imaging. Table.1 demonstrates the suggested model's ability to classify various stages of gastric cancer.

Table 1. Performance Evaluation of the Proposed Model

Classes	Accuracy	Precision	Recall	Specificity	F1 score
Normal	99.07	98.24	96.65	96.08	97.32
Abnormal	99.17	97.02	98.74	95.17	98.05

Table 1 shows the suggested model's usefulness in categorizing various kinds of lung cancer, such as normal and atypical instances. The suggested model achieves an accuracy of 99.12% for the LIDC-IDRI [17] dataset. Furthermore, the suggested model has overall precision, recall, specificity, and F1 scores of 97.63%, 97.69%, 95.62%, and 97.68%, respectively.

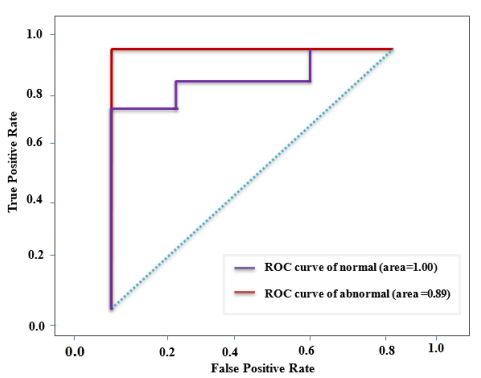


Figure 4. ROC curve of the proposed model

Figure 4 depicts the ROC computed for various lung cancer groups. The obtained CT dataset achieves a higher AUC. The suggested model produced an AUC of 0.1 for normal instances and 0.89 for abnormal cases, as assessed by the TPR and FPR parameters.

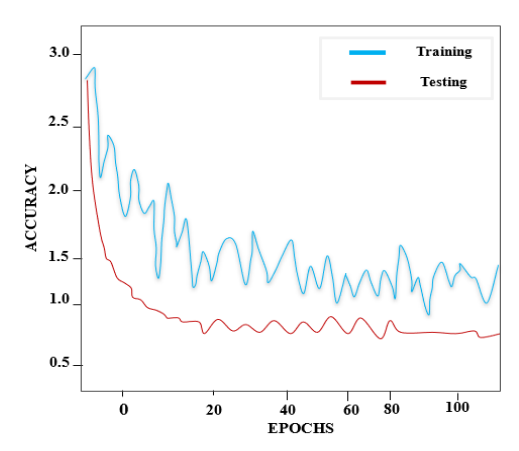


Figure 5. Accuracy curve of the proposed model

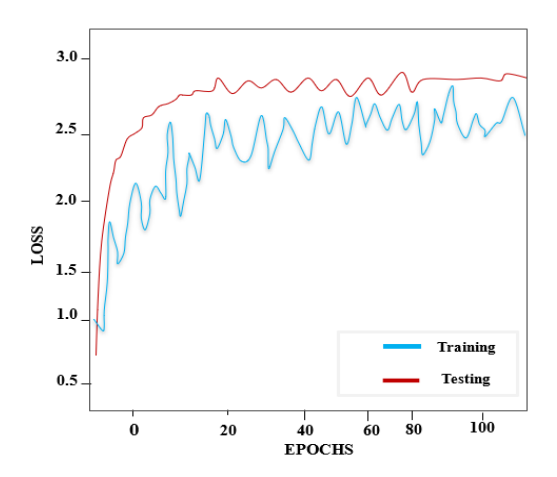


Figure 6. Loss curve of the proposed model

In Figure.5, The accuracy graph has been calculated using 100 epochs and an accuracy range. When the total amount of epochs increases, the accuracy for the suggested model improves. Figure 6 depicts the epochs and loss range, revealing that as the epochs increase, the loss of the suggested model reduces. The suggested approach achieves great accuracy in the identification of the various stages of stomach cancer using CT scans.

4.2. Comparative analysis

The effectiveness of each neural network was evaluated to ensure that the results of the proposed model are accurate. Competence evaluation was conducted between the proposed model and deep learning classifiers such as Alex Net, Google Net, and ResNet. The suggested model achieves 99.12% accuracy, which exceeds that of traditional DL networks.

According to Table 2. The suggested Link Net has a higher accuracy than classic networks such as Alex Net, Google Net, and ResNet. Link Net maintains 99.12% high accuracy ranges. Link Net achieves an accuracy rate that is more efficient than that of existing approaches. The suggested Link Net improves accuracy by 2.43%, 4.89%, and 1.98% compared to Alex Net, Google Net, and ResNet, respectively.

Table 2. Compared to conventional deep learning networks

Techniques	Accuracy	Specificity	Precision	Recall	F1 score
Alex Net	96.69	94.84	90.31	94.29	95.87
Google Net	94.23	95.59	93.51	94.67	94.43
ResNet	97.14	93.48	95.19	95.78	96.79
Proposed Link Net	99.12	95.62	97.63	97.69	97.68

According to Table 3, the proposed model enhances the overall accuracy of 2.44%, 5.04% and 4.34% better than CNN, faster R-CNN, and VGG-16 CNN respectively.

According to the comparison above, the proposed model method is more reliable than existing models.

Table 3. Comparison between the suggested model and the existing models

Authors	Techniques	Accuracy
Horiuchi, et al [11]	CNN	85.3%
Wang, and Liu, [12]	DeepLab v3+	91.66%
Chen, et al [13]	GHID	97.97%
Proposed method	Link Net	99.12%

5. CONCLUSION

In this paper GADDLE technique has been proposed to identify the gastric cancer in an CT image. Initially the input images are pre-processed using the Gaussian adaptive bilateral filter to enhance the quality of the image. Then the pre-processed images are fed into RegNet feature extraction model to for extracting the features in the image. The best features are selected by using the Dingo Optimization Algorithm. Finally, the normal and the abnormal case of the GC are classified using Link Net model. The GasHisSDB datasets are used to evaluate the performance of the proposed method of specific matrices such as Specificity, Recall, Accuracy, Precision and F1-Score. The suggested Link Net improves accuracy by 2.43%, 4.89%, and 1.98% compared to Alex Net, Google Net, and ResNet. In future this research focus on AI-driven image analysis combined with physical biomarkers for more accurate stomach cancer detection.

CONFLICTS OF INTEREST

The authors declare that they have no known competing financial interests or personal relationships that could have appeared to influence the work reported in this paper.

FUNDING STATEMENT

Not applicable.

ACKNOWLEDGEMENTS

The author would like to express his heartfelt gratitude to the supervisor for his guidance and unwavering support during this research for his guidance and support.

REFERENCES

- [1] Z. Song, S. Zou, W. Zhou, Y. Huang, L. Shao, J. Yuan, X. Gou, W. Jin, Z. Wang, X. Chen, and X. Ding, "Clinically applicable histopathological diagnosis system for gastric cancer detection using deep learning", *Nature communications*, vol. 11, no. 1, pp.4294, 2020. [CrossRef] [Google Scholar] [Publisher Link]
- [2] A.P. Thrift, and H.B. El-Serag, "Burden of gastric cancer", *Clinical Gastroenterology and Hepatology*, vol. 18, no. 3, pp.534-542, 2020. [CrossRef] [Google Scholar] [Publisher Link]
- [3] S.S. Joshi, and B.D. Badgwell, "Current treatment and recent progress in gastric cancer", *CA: a cancer journal for clinicians*, vol. 71, no. 3, pp. 264-279, 2021. [CrossRef] [Google Scholar] [Publisher Link]

- [4] J.W. Chae, and H.C. Cho, "Enhanced Classification of Gastric Lesions and Early Gastric Cancer Diagnosis in Gastroscopy Using Multi-Filter Auto Augment", *IEEE Access*, vol. 11, pp. 29391-29399, 2023. [CrossRef] [Google Scholar] [Publisher Link]
- [5] Z. Wang, Y. Liu, and X. Niu, "Application of artificial intelligence for improving early detection and prediction of therapeutic outcomes for gastric cancer in the era of precision oncology", *In Seminars in Cancer Biology*. Academic Press. 2023. [CrossRef] [Google Scholar] [Publisher Link]
- [6] L. Liu, Z. Dong, J. Cheng, X. Bu, K. Qiu, C. Yang, J. Wang, W. Niu, X. Wu, J. Xu, and T. Mao, "Diagnosis and segmentation effect of the ME-NBI-based deep learning model on gastric neoplasms in patients with suspected superficial lesions-a multicenter study", Frontiers in Oncology, vol. 12, pp.1075578, 2023. [CrossRef] [Google Scholar] [Publisher Link]
- [7] Z. Zhang, and J. Peng, "Clinical nursing and postoperative prediction of gastrointestinal cancer based on CT deep learning model", *Journal of Radiation Research and Applied Sciences*, vol. 16, no. 2, pp.100561, 2023. [CrossRef] [Google Scholar] [Publisher Link]
- [8] W. Ba, S. Wang, M. Shang, Z. Zhang, H. Wu, C. Yu, R. Xing, W. Wang, L. Wang, C. Liu, and H. Shi, "Assessment of deep learning assistance for the pathological diagnosis of gastric cancer", *Modern Pathology*, vol. 35, no. 9, pp.1262-1268, 2022. [CrossRef] [Google Scholar] [Publisher Link]
- [9] M.R. Afrash, E. Mirbagheri, M. Mashoufi, and H. Kazemi-Arpanahi, "Optimizing prognostic factors of five-year survival in gastric cancer patients using feature selection techniques with machine learning algorithms: a comparative study", BMC Medical Informatics and Decision Making, vol. 23, no. 1, pp.54, 2023. [CrossRef] [Google Scholar] [Publisher Link]
- [10] L. Li, Y. Chen, Z. Shen, X. Zhang, J. Sang, Y. Ding, X. Yang, J. Li, M. Chen, C. Jin, and C. Chen, "Convolutional neural network for the diagnosis of early gastric cancer based on magnifying narrow band imaging", *Gastric Cancer*, vol. 23, pp.126-132, 2020. [CrossRef] [Google Scholar] [Publisher Link]
- [11] Y. Horiuchi, K. Aoyama, Y. Tokai, T. Hirasawa, S. Yoshimizu, A. Ishiyama, T. Yoshio, T. Tsuchida, J. Fujisaki, and T. Tada, "Convolutional neural network for differentiating gastric cancer from gastritis using magnified endoscopy with narrow-band imaging", *Digestive diseases and sciences*, vol. 65, pp.1355-1363, 2020. [CrossRef] [Google Scholar] [Publisher Link]
- [12] J. Wang, and X. Liu, "Medical image recognition and segmentation of pathological slices of gastric cancer based on Deeplab v3+ neural network," *Computer Methods and Programs in Biomedicine*, vol. 207, pp.106210, 2021. [CrossRef] [Google Scholar] [Publisher Link]
- [13] H. Chen, C. Li, G. Wang, X. Li, M.M. Rahaman, H. Sun, W. Hu, Y. Li, W. Liu, C. Sun, and S. Ai, "GasHis-Transformer: A multi-scale visual transformer approach for gastric histopathological image detection", *Pattern Recognition*, vol. 130, pp.108827, 2022. [CrossRef] [Google Scholar] [Publisher Link]
- [14] S.A. Lee, H.C. Cho, and H.C. Cho, "A novel approach for increased convolutional neural network performance in gastric-cancer classification using endoscopic images", *IEEE Access*, vol. 9, pp.51847-51854, 2021. [CrossRef] [Google Scholar] [Publisher Link]
- [15] F. Su, J. Li, X. Zhao, B. Wang, Y. Hu, Y. Sun, and J. Ji, "Interpretable tumor differentiation grade and microsatellite instability recognition in gastric cancer using deep learning", *Laboratory Investigation*, vol. 102, no. 6, pp.641-649, 2022. [CrossRef] [Google Scholar] [Publisher Link]

- [16] L. Wu, J. Wang, X. He, Y. Zhu, X. Jiang, Y. Chen, Y. Wang, L. Huang, R. Shang, Z. Dong, and B. Chen, "Deep learning system compared with expert endoscopists in predicting early gastric cancer and its invasion depth and differentiation status (with videos)", Gastrointestinal Endoscopy, vol. 95, no. 1, pp.92-104, 2022. [CrossRef] [Google Scholar] [Publisher Link]
- [17] M.P. Yong, Y.C. Hum, K.W. Lai, Y.L. Lee, C.H. Goh, W.S. Yap, and Y.K. Tee, "Histopathological Gastric Cancer Detection on GasHisSDB Dataset Using Deep Ensemble Learning", *Diagnostics*, vol. 13, no. 10, pp.1793, 2023. [CrossRef] [Google Scholar] [Publisher Link]

AUTHORS



R. Tharani she was born in Kanyakumari District, Tamil Nadu, India in 1999. She received her B.E degree in computer science and Engineering from Arunachal college of engineering, Manavilai, Anna University. Indian in 2022. Currently she is pursuing her M.E degree in computer science and engineering, Manavilai, Anna University. Indian. Her interested area is Image Processing and Internet of Things



C. Jasphin received her B.E degree in CSE from St. Xavier's Catholic College, chunkankadai in 2010, and she obtained her M.E degree in CSE from St. Xavier's Catholic College, Chunkankadai in 2012.she persuing her Ph.D. degree for her research work on medical image. Currently she is working as an Assistant professor in the department of CSE Arunachal college of engineering for women, India. Her research area of interest includes Cloud

computing, Image Processing, Internet of Things

Arrived: 10.05.2024 Accepted: 05.06.2024



RESEARCH ARTICLE

DNA ENCRYPTION-BASED SECURE ACCESS CONTROL AND DATA SHARING IN AN ENABLED CLOUD ENVIRONMENT

A.R. Aarthy 1, * and K. Vinoth Kanth 2

¹ Department of Computer Science and Engineering, Satyam College of Engineering and Technology, Aralvaimozhi, Anna University, India.

² Department of Computer Science and Engineering, University college of engineering Nagercoil, India.

*Corresponding e-mail: aarthyvishnu343@gmail.com

Abstract - IoT and cloud service providers are vulnerable to both internal and external threats consequently it is not possible to fully trust them with sensitive customer data. The cloud should offer a mechanism for the user to verify if the integrity of his data is being maintained or if it has been compromised, as the user cannot physically judge the data. Cloud computing is the best solution for storing this type of data. IoT has introduced secure data sharing and access management to prevent this issue. However, centralized access control presents a number of difficulties. The goal is to develop a novel DNA Encryption-based Secure Access Control and Sharing (DESACS) technique that has been proposed in an IoT-enabled Cloud environment which enhances the privacy and security of IoT data. The privacy of IoT has been increased by encrypting the data using the DNA cryptography (DNAC) encryption technique. It offers fresh hope for breaking invincible algorithms. This is a result of DNA computing's increased speed, low storage needs, and power consumption. In contrast to traditional storage media, which require 1012 nm3/bit, DNA stores memory at a density of roughly 1 bit/nm3.

Keywords – Internet of Things, DNA, Cloud, DNA Encryption.

1. INTRODUCTION

ISSN: xxxx-xxxx

The development of Internet of Things (IoT) technology has made it possible for several things to communicate with one another, opening up a variety of applications such as smart manufacturing, smart transportation, and smart housing [1]. Sharing data has become a standard practice for individuals, scientific groups, educational institutions, and the medical business. IoT has seen a sharp rise in demand, acceptance, and commercial availability in the last few years [2]. The IoT is vulnerable to the leakage of private information during data exchange. Medical data is critical to patient care, research, and public health. It provides critical information to healthcare professionals, allowing them to make informed decisions about diagnosis and treatment, while also funding research efforts to better understand diseases, develop new therapies, and improve patient outcomes [3]. Data exchange both inside and outside of organizations is essential for industries and financial

institutions [4]. A wide network with a number of IoT-enabled apps and devices makes up the cloud architecture based on the Internet of Things [5].

Cloud computing is the process of delivering computation and resources over the internet as a service rather than a product, enabling users to access databases, information, hardware, software, and other resources anytime they're needed [6]. Consumers utilize on-demand services and pay for them without taking into account the initial expenses of infrastructure and ongoing maintenance [7]. Cloud computing has gained significant attention recently and is growing in popularity as a result of these benefits [8]. These days, there are numerous cloud service providers, including Microsoft Azure, Amazon EC2, and others [9]. Considering their vulnerability to both internal and outsider assaults, cloud and IoT service companies cannot be completely trusted with sensitive personal data [10]. The cloud should offer a way for the user to ascertain whether the integrity of his data is preserved or jeopardized because the data is not physically available to consumers [11]. Cloud computing is the best way to store this type of data. One major problem is the lack of interoperability between different IoT devices and apps on the cloud design. To address this issue, a novel DNA Encryption-based Secure Access Control and Sharing (DESACS) technique that has been proposed in an IoT-enabled Cloud environment which enhances the privacy and security of IoT data.

2. LITERATURE REVIEW

In 2020 Rashid, et al. [12] proposed the implementation of Internet of Things medical data stored on public cloud platforms in healthcare systems is secured using Enhanced Role Based Access Control (ERBAC). A secure cloud system for storing medical data based on role-based access policies will be made possible by the suggested system it will also significantly aid in the efficient storage of medical data from online applications. This model provides the required

limitations on responsibilities and uses to guarantee the safety of health information kept on cloud-based platforms.

In 2021 Shi, et al. [13] proposed DUCE, a distributed employ control enforcement approach for CEIoT data exchange. The suggested approach makes use of Trusted Execution Environment (TEE) and blockchain technology to provide dependable and continuous enforcement of the cross-domain data-sharing lifecycle. Comparing the findings to OAuth 2.0, the performance and scalability overhead are tolerable. An open-source permissioned blockchain system prototype is being evaluated through the experimental deployment.

In 2022 Kitagawa, et al. [14] proposed SINETStream a method for sharing and safely encrypting data using a Secure Configuration Server. Confidential information is given to recipients through the mechanism in an encrypted manner restricting access to only those that are permitted. This approach makes it simple to share sensitive data since it securely manages data encryption keys within the system, something that traditional systems have made difficult.

In 2023 Fugkeaw, et al. [15] developed LightMED, an access control system that combines blockchain, CP-ABE, and fog computing to enable safe, scalable, and fine-grained EMR sharing in a cloud-based environment. It conducted trials to evaluate our plan's and related works' efficacy and finished a comparative analysis to illustrate the computation cost. The design suggests a mechanism for securely transmitting and aggregating IoT data that is based on digital signing and lightweight encryption. The method's principal addition includes an access policy mechanism that protects privacy along with outsourced encryption.

In 2023 Liu, et al. [16] proposed BP-AKAA, a attributebased access control made possible by a key agreement method and cross-domain private-protected authentication implemented by blockchain technology. Device identities are safeguarded by the use of non-interactive zero-knowledge proof technology. Performance investigation indicates that this method outperforms current approaches in terms of access control, authentication, and key generation. It also fulfills a number of requirements including as mutual authentication, privacy preservation, and cross-domain functionality.

In 2023 Han, et al. [17] introduced a blockchain-based, internal product encryption-based Internet of Things access management method. Inner product encryption provides fine-grained access control, complete concealment of access limitations, and data security and user privacy for lightweight Iot devices by utilizing the property of vector representation of characteristics. The mechanism can match the specific access control requirements of the Internet of Things and has great efficiency while guaranteeing security, according to the experimental findings.

In 2024 Singh, et al. [18] proposed the DNACDS access control model and cryptography technique to solve the massive data security and access issues in the Internet of Everything. Deoxyribonucleic acid (DNA) computing is a biological idea that potentially enhances Internet of Everything (IoE) large data security. The suggested method outperforms other DNA-based security systems, as demonstrated by the experimental results. Better resistance capabilities are revealed by the DNACDS's theoretical security research.

3. PROPOSED METHOD

In this section a novel DNA Encryption-based Secure Access Control and Sharing (DESACS) technique that has been proposed in an IoT-enabled Cloud environment which enhances the privacy and security of IoT data. The privacy of IoT has been increased by encrypting the data using the DNA cryptography (DNAC) encryption technique (Figure 1).

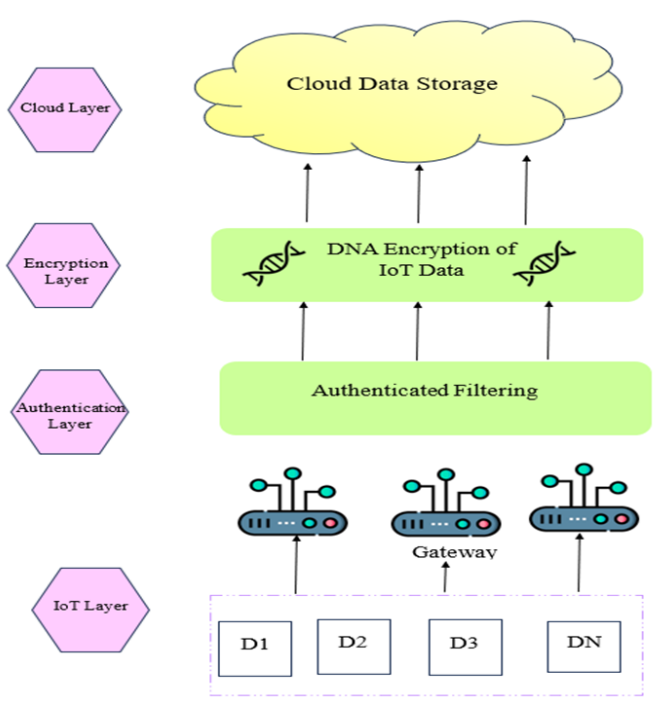


Figure 1. Block diagram of proposed DESACS technique

3.1. IoT Layer

The IoT layer represents the foundation of the system where various Internet of Things (IoT) devices, labelled from D1 to DN, are interconnected. The data collection and transmission to the gateways is the responsibility of these devices from their respective contexts. The depiction of multiple devices suggests a scalable network capable of handling a range of IoT devices, each potentially monitoring different parameters or performing distinct functions. This layer is crucial as it serves as the data source for the subsequent security and storage processes in the system's architecture.

3.2. Authentication Layer

The authentication layer serves as the gatekeeper to a system, verifying the identity of users and granting access to authorized individuals or entities. This layer guards against unauthorized access and potential security risks while guaranteeing that only authorized users are given access to the system's resources and services.

3.2.1. Authentication-Based Request Filtration

Through the GW, users can submit a request message to the EN for real-time access to the IoT devices. Request filtration is carried out by the GW to lessen DDoS assaults brought on by unauthorized user requests. First, the GW uses filters to confirm the legitimacy of the users that created the requests. The filter initially begins with an m-bit empty array. When the element's eligibility for the filter is confirmed, it returns false. The element must first be approved by the hash function in order to be added to the filter. In this instance, hashing is done using the SHA-256 technique. The result of the hash function is used to determine a location in the filter's array. One is assigned to the bit's location. The places in the filter are created using hash functions, which are then used to check the element in the filter. The filter indicates that the request is valid if every position in the array is one; if not, it is invalid. Therefore, to validate the elements in the array, the hash function is employed. Furthermore, it serves to confirm the request's validity. The definition of the filter's false positive rate (σ) for large values of m is as follows:

$$\sigma = (1 - a^{-\frac{ep}{k}})^e \tag{1}$$

where e and p stand for the false positive rate, e for the nearest power 2 value, and p is rounded to the closest integer value. The number of elements in the filter is indicated by Q. It only filters valid requests based on the filter. The timestamp and freshness of the arriving packets are checked to make sure the user is authentic. This will screen and ignore the unauthorized access requests that are triggering denial-of-service attacks. The load on access delegation is lessened because only valid access requests are handled.

3.3. Encryption Layer

The encryption layer serves as a crucial component of security infrastructure, safeguarding data by converting it into an unreadable format using cryptographic algorithms. This layer ensures the confidentiality and integrity of information transmitted or stored within a system by encoding data into ciphertext, meaning that only people with

the right authorization and decryption keys may decode it. This uses DNA encryption to encrypt the IoT data.

3.3.1. DNA encryption

The unique storage density of DNA as an information carrier makes it a better option for handling the challenge of producing or storing massive amounts of Pad. Utilizing DNA as an information carrier and contemporary biological processes as instruments, DNA cryptography fully utilizes the inherent benefits of high storage density and high parallelism to produce encryption. It is possible to replicate the encryption and decryption process as a biological or chemical reaction based on the double helix structure of DNA and the Watson-Crick complementary principle. After a substantial operation, it encodes the data and stores the plaintext, ciphertext, or other information on DNA encoding nucleotide sequence. The password mechanism has been developed by this point. Because so many DNA-based encryption algorithms have been developed in recent years, DNA cryptography is still in its infancy and lacks a comprehensive model and an effective verification method.

3.3.2 Key Select and the Plaintext Block

Key Select

The key in this encryption might be split into two pieces. (1). The selected gene sequence information, which is one component of the key, will be communicated over a secure channel between the sender and the recipient and will not be accessible to outside parties. The researcher establishes the beginning and ending points of the search position to improve algorithm security. The advantage of this approach is that it eliminates the requirement for entire gene sequence expression, and it saves money by limiting encryption and decryption operations to the crucial location of the key sequence from the point at which both parties agreed to begin. (2). As an additional component of the key, the Key Generator's beginning key is used to operate the device and produce a chaotic sequence. The two parameters μ and x in this section represent the key, as the Key Generator we built is based on Logistic Mapping.

Plaintext Block

The binary plaintext needs to be grouped into 32-bit chunks before encryption. When "GENEGRYPTOGRAPHY" is the plaintext, for instance, Group 1 will be "GENE", Group 2 will be "GRYP", Group 3 will be "TOGR", and Group 4 will be "APHY" until the plaintext is blocked. The plaintext ought to be filled in when its length is not divisible by four. The specific operation is as follows: We fill in the remaining space at the end of the plaintext after Mod 4. For example, we will insert three letters "3" at the end of the plaintext when the length of the plaintext mod 4 equals 3.

3.3.3 Encryption

Step 1: The investigator determines at random the Initial Key key0, which consists of two double values, and sets them as the Logistic Mapping parameters (μ and x); In addition, the first encryption will use a 32-bit key1 generated by the Key Generator to encrypt plaintext. Then, following

converting plaintext into ASCII codes, the researchers should separate the participants into various groups; Lastly, the researcher ought to do an XOR operation between key1 and the 32-bit plaintext. The sequence m1 will be obtained by the researcher following these steps.

Step 2: Initially m1 needs to be translated into DNA code in accordance with the DNA encoding described in 3.1. The researcher will obtain the 16-mer olio nucleotide DNA sequence se1 through encoding; Second, the unique DNA sequence (DNAseq) included in them will be obtained using the key and the provided DNA sequence information; Next, the researcher draws a random point x (0<x), from which the special string that matches m1 is found by searching the sequence. Four continuous bases mean that se11, se12, se13, and se14 can all be exactly the same as m1. The following will be returned: q1, q2, q3, q4; The points are then restored into the cipher-text array Pointer by the method.

Step 3: A new encryption key key_m is generated by the Key Generator and is utilized in the subsequent encryption procedure. Moreover, the researcher ought to do an XOR operation on the 32-bit plaintext and key_m . Then, the new sequence n_m will appear.

Step 4: Steps two and three should be carried out continuously until all plaintext has been encrypted. At that point, the program can be terminated. The process of decryption is the opposite of that of encryption.

3.3.4. DNA Symmetric Encryption Cryptosystem

Data including keys and DNA sequences should be sent over the secure channel by both the sender and the recipient. Sender uses a public channel to transmit ciphertext to the recipient. The receiver will utilize the DNA sequence information to determine the correct DNA sequence after receiving the cipher-text from the sender. The proper plaintext will then be retrieved by the recipient using the key and the decryption method.

3.3.5. Key Generator

1. Developing Chaos Sequence y: The key is provided by the values of the logistic parameters τ and x. The chaos sequence will be produced using formula 2:

$$y = (y1, y2, y3, ..., yk)$$
 (2)

2. Creating Key: The key yj will be chosen in the sequence y for each round. Formula (3) states that it will be changed into a 32-bit binary number:

$$[zj]2 = yj9 * 255 (3)$$

3.Consequently, in each round, the key Z will be represented by formula (4):

$$z = [zj, zj + 1, zj + 2, zj + 3]$$
(4)

Reason: the chaotic sequence y is where the chaos value yj originated. 255 must be multiplied before it maps to 8-bit binary zj. Each consecutive four zj will be utilized as a single 32-bit key.

3.4. Cloud Layer

The cloud layer refers to the virtualized infrastructure that enables the delivery of computing services over the Internet. The part of the cloud computing infrastructure devoted to safely storing and managing data is referred to as the cloud data storage layer. It includes databases and distributed storage systems spread across several servers and data centres, offering scalable, dependable, and reasonably priced storage solutions. In this, the DNA-encrypted IoT datas are stored in the cloud layer.

4. RESULT AND DISCUSSION

The proposed method's experimental results are analyzed and discussion of performance is done in terms of numerous evaluation metrics in this section. The effectiveness of the proposed system has been assessed by using the MATLAB simulator with a 4 GB RAM and an i5 processor.



Figure 2. Home Page

Figure 2 shows the homepage. It is the home page of the DNA Encryption based Secure access control and Data sharing in an enabled cloud environment.



Figure 3. User Registration

Figure 3. shows the user registration page of the DNA Encryption based Secure access control and Data sharing in an enabled cloud environment in which the user gives the details for registration.

Figure 4 describes the Decrypted web page of the DNA Encryption based Secure access control and Data sharing in an enabled cloud environment

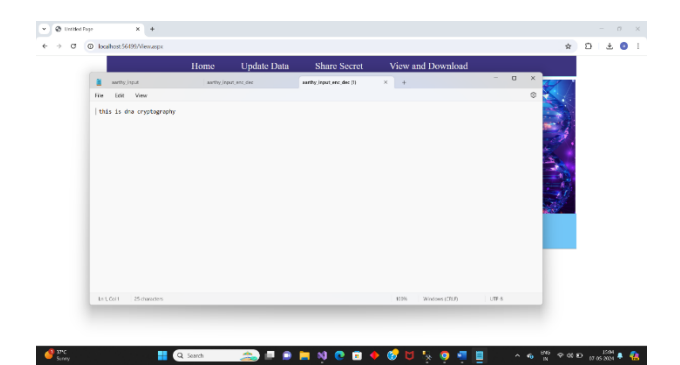


Figure 4. Decrypted web page

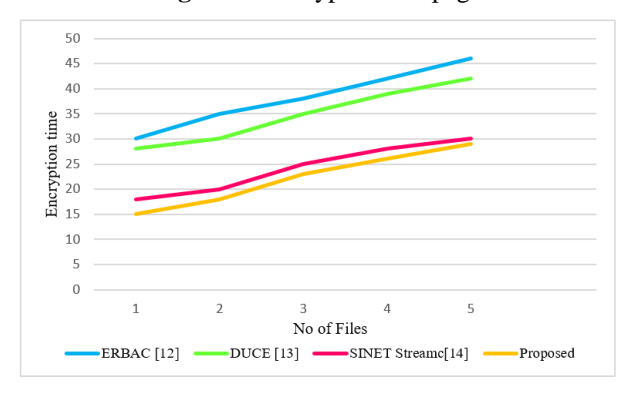


Figure 5. Comparison Analysis of Encryption Time

The encryption time of the proposed DESACS technique is compare with the existing methods. In this, the proposed DESACS technique takes less time to encrypt a file than the existing methods such as ERBAC [12], DUCE [13] and SINET Stream [14]. The proposed technique's encryption time is 72.07%, 56.92%, and 9.04% faster than that of the existing methodologies (Figure 5).

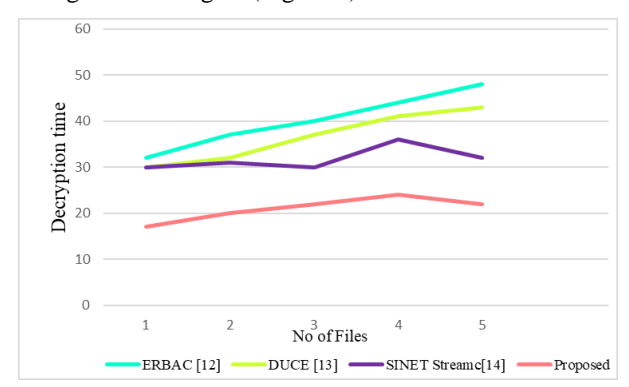


Figure 6. Comparison Analysis of Decryption Time

Figure 6. describes the decryption time comparison of the proposed DESACS with the existing method. The proposed method takes less time consumption than the existing methods. The decryption time of the proposed technique is 82.7%, 63.36%, and 19.09% faster than that of the existing techniques.

In Figure. 7, the proposed system and the existing techniques such as ERBAC [12], DUCE [13], and SINET Stream [14] are contrasted for the execution time. In this, the proposed DESACS takes less time for execution than the existing methods.

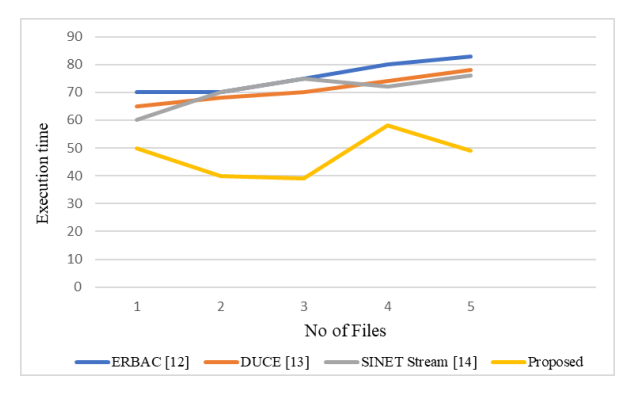


Figure 7. Comparison Analysis Execution time

5. CONCLUSION

A DNA Encryption-based Secure Access Control and Sharing (DESACS) technique in an IoT-enabled Cloud environment which enhances the privacy and security of IoT data. Initially, the IoT layer represents the devices in the Internet of Things (IoT) ecosystem. These devices (labelled D1 to DN) are connected to gateways. The gateways act as intermediaries, facilitating communication between the devices and other layers. Then the Authentication is a crucial step to ensure that only authorized devices and data can proceed further. The pink hexagon labelled "Authenticated Filtering" likely represents a mechanism for verifying the identity of devices or data streams. Devices that pass authentication can move on to the next layer. The Data encryption improves data security. Data might have been encrypted using DNA sequences in a process known as "DNA-based encryption," which would be challenging to decode without the right key. Finally, the top layer Cloud data storage provides scalability, accessibility, and redundancy. The proposed secure data transmission scheme will be extended to work in an uncontrolled environment in future by replacing increasing security challenges in cloud computing while ensuring data confidentiality and privacy in a globally connected digital ecosystem.

CONFLICTS OF INTEREST

The authors declare that they have no known competing financial interests or personal relationships that could have appeared to influence the work reported in this paper.

FUNDING STATEMENT

Not applicable.

ACKNOWLEDGEMENTS

The author would like to express his heartfelt gratitude to the supervisor for his guidance and unwavering support during this research for his guidance and support.

REFERENCES

- [1] P. Goyal, A.K. Sahoo, and T.K. Sharma, "Internet of things: Architecture and enabling technologies", Materials Today: Proceedings, vol. 34, pp.719-735, 2021. [CrossRef] [Google Scholar] [Publisher Link]
- [2] L. Kong, and B. Ma, "Intelligent manufacturing model of construction industry based on Internet of Things technology", The International Journal of Advanced Manufacturing Technology, vol. 107, no. 3, pp.1025-1037, 2020. [CrossRef] [Google Scholar] [Publisher Link]

- [3] E. Bazgir, E. Haque, N.B. Sharif, and M.F. Ahmed, "Security aspects in IoT based cloud computing", World Journal of Advanced Research and Reviews, vol. 20, no. 3, pp.540-551, 2023. [CrossRef] [Google Scholar] [Publisher Link]
- [4] S. Nguyen, Z. Salcic, X. Zhang, and A. Bisht, "A low-cost twotier fog computing testbed for streaming IoT-based applications", *IEEE Internet of Things Journal*, vol. 8, no. 8, pp.6928-6939, 2020. [CrossRef] [Google Scholar] [Publisher Link]
- [5] N. Muthukumaran, N. Ruban Guru Prasath, R. Kabilan, "Driver Sleepiness Detection Using Deep Learning Convolution Neural Network Classifier", *Third International* conference on I-SMAC (IoT in Social, Mobile, Analytics and Cloud), Palladam, India, pp. 386-390, 2019. [CrossRef] [Google Scholar] [Publisher Link]
- [6] A.T. Atieh, "The next generation cloud technologies: a review on distributed cloud, fog and edge computing and their opportunities and challenges", ResearchBerg Review of Science and Technology, vol. 1, no. 1, pp.1-15, 2021. [CrossRef] [Google Scholar] [Publisher Link]
- [7] R. Joshua Samuel Raj, T. Sudarson Rama Perumal, N. Muthukumaran, D.R. Ganesh, "Rapid Efficient Loss Less Color Image Compression Using RCT Technique and Hierarchical Prediction", In: Peter, J.D., Fernandes, S.L., Alavi, A.H. (eds) "Disruptive Technologies for Big Data and Cloud Applications", Lecture Notes in Electrical Engineering, vol. 905, pp. 189–202, 2022. [CrossRef] [Google Scholar] [Publisher Link]
- [8] F. Jauro, H. Chiroma, A.Y. Gital, M. Almutairi, M.A. Shafi'i, and J.H. Abawajy, "Deep learning architectures in emerging cloud computing architectures: Recent development, challenges and next research trend", *Applied Soft Computing*, vol. 96, pp.106582, 2020. [CrossRef] [Google Scholar] [Publisher Link]
- [9] B. Alouffi, M. Hasnain, A. Alharbi, W. Alosaimi, H. Alyami, and M. Ayaz, "A systematic literature review on cloud computing security: threats and mitigation strategies", *IEEE Access*, vol. 9, pp. 57792-57807, 2021. [CrossRef] [Google Scholar] [Publisher Link]
- [10] A. Karthika, N. Muthukumaran, and R. Joshua Samuel Raj, "An Ads-Csab Approach for Economic Denial of Sustainability Attacks in Cloud Storage", *International Journal of Scientific & Technology Research*, vol. 9, no. 04, pp. 2575-2578, 2020. [CrossRef] [Google Scholar] [Publisher Link]
- [11] G. Deep, J. Sidhu, and R. Mohana, "Insider threat prevention in distributed database as a service cloud environment", *Computers & Industrial Engineering*, vol. 169, pp.108278, 2022. [CrossRef] [Google Scholar] [Publisher Link]
- [12] M. Rashid, S.A. Parah, A.R. Wani, and S.K. Gupta, "Securing E-Health IoT data on cloud systems using novel extended rolebased access control model", *Internet of Things (IoT) Concepts* and Applications, pp.473-489, 2020. [CrossRef] [Google Scholar] [Publisher Link]

- [13] N. Shi, B. Tang, R. Sa ndhu, and Q. Li, "DUCE: distributed usage control enforcement for private data sharing in the Internet of Things", *In Data and Applications Security and Privacy XXXV*: 35th Annual IFIP WG 11.3 Conference, DBSec 2021, Calgary, Canada, July 19–20, 2021, Proceedings 35, pp. 278-290, 2021. [CrossRef] [Google Scholar] [Publisher Link]
- [14] N. Kitagawa, A. Takefusa, and K. Aida, "Development of a Secure Data Sharing Mechanism for IoT Application Systems", In 2022 IEEE 11th International Conference on Cloud Networking (CloudNet), pp. 131-135, 2022. IEEE. [CrossRef] [Google Scholar] [Publisher Link]
- [15] S. Fugkeaw, L. Wirz, and L. Hak, "Secure and Lightweight Blockchain-enabled Access Control for Fog-Assisted IoT Cloud-based Electronic Medical Records Sharing", IEEE Access. 2023. [CrossRef] [Google Scholar] [Publisher Link]
- [16] S. Liu, L. Chen, H. Yu, S. Gao, and H. Fang, "BP-AKAA: blockchain-enforced privacy-preserving authentication and key agreement and access control for IoT", *Journal of Information Security and Applications*, vol. 73, p.103443, 2023. [CrossRef] [Google Scholar] [Publisher Link]
- [17] P. Han, Z. Zhang, S. Ji, X. Wang, L. Liu, and Y. Ren, "Access control mechanism for the Internet of Things based on blockchain and inner product encryption", *Journal of Information Security and Applications*, vol. 74, pp.103446, 2023. [CrossRef] [Google Scholar] [Publisher Link]
- [18] A. Singh, A. Kumar, and S. Namasudra, "DNACDS: Cloud IoE big data security and accessing scheme based on DNA cryptography", Frontiers of Computer Science, vol. 18, no. 1, pp.181801, 2024. [CrossRef] [Google Scholar] [Publisher Link]

AUTHORS



A.R. Aarthy she was born in Kanyakumari district, Tamil Nadu, India in 1999. She received her BE degree in Computer Science and Engineering from Satyam college of Engineering and Technology, Aralvaimozhi, Anna University, currently she is pursuing her ME degree in Computer Science and Engineering from

Satyam College of Engineering and Technology, Aralvaimozhi, Anna University, India. Her interested research area is cloud computing, and Internet of Things.



K. Vinoth Kanth received his B.tech in Information Technology from Sun college of engineering and technology, Anna University, in 2009 and obtained M.E degree in CSE from University college of engineering Nagercoil in 2013. His interested research area is Image processing and cloud computing.

Arrived: 17.05.2024 Accepted: 08.06.2024



RESEARCH ARTICLE

IT EMPLOYEES STRESS DETECTION BASED ON YOLO DEEP LEARNING ALGORITHM

S. Abinisha ^{1,*} and S. S. Pooja ²

¹Department of Computer Science and Engineering Engineering, Satyam College of Engineering and Technology, Aralvaimozhi, Anna University, Chennai, India.

² Department of Computer Science and Engineering, Loyola Institute of Technology & Science, Loyola Nagar, Thovalai, Rajavoor Road, Kanyakumari, India.

*Corresponding e-mail: abinishas2001@gmail.com

Abstract - Stress related disorders are extremely prevalent among workers in the corporate sector. The high demands and extended work hours of IT employment have led to an increase in stress among IT workers. In this paper a novel STress DEtection on it employees using YOLO deep learning (STEP-YOLO) has been proposed for detecting the Stress on IT Employees. Initially, the input images are pre-processed in this pre-processing image acquisition and image processing are done to enhance the image. The features are extracted from the pre-processed image it extracts the feature whether they are happy, sad or neutral. Finally, the objects are detected using the YOLOv5 technique to detect the stress on IT employees. The proposed STEP-YOLO achieves an accuracy rate of 99.35% and an overall accuracy rate of 0.94%, 1.61% and 0.7% which is comparatively higher than the existing methods such as UBFC-Phys, PSS and SAD. The proposed method takes 0.18 milliseconds to detect the stress on IT employees which is comparatively less than the existing methods respectively.

Keywords – YOLOv5, Deep Learning, Stress Detection, IT Employees.

1. INTRODUCTION

ISSN: xxxx-xxxx

One of the main manifestations of human life is stress. Stress plays a significant part in people's lives [1]. Numerous illnesses, including cancer, heart disease, lung issues, breathing difficulties, and other conditions, can be brought on by stress [2]. The growth in global population has led to a rise in people's stress levels. Stress is a prevalent condition among all people these days. Systems for managing stress are essential for identifying stress levels that impact our socioeconomic status [3]. A quarter of the population experiences mental health problems, such as stress, as per the World Health Organization (WHO) [4]. Human stress manifests as mental and financial difficulties, unclear thinking at work, poor working relationships, hopelessness, and, in severe cases, death [5]. The IT industry is always introducing new products and services in order to stay competitive. Furthermore, this poll indicates that over the previous year, employees' stress levels have increased [6]. Even though many businesses offer their employees advantages related to mental health, the issue still exists. We'll start by examining how stressed-out workers are at work [7]. The investigation will employ machine learning and images to analyze stress patterns and identify the key variables affecting each person's stress threshold. One in four voters suffer from stress, a mental illness, according to the WHO [8].

Employers can better educate their staff to handle stressful situations before they arise by implementing the Stress Detection System. Stress identification may occasionally require differentiating between a "stressed" and a "relaxed" situation, even while office workers are focused on their work [9]. Employees have their heads photographed, and they receive survey questions with a similar standard format and style. There is less physical strain, which results in time and cost savings [10]. Using our laboriously created questionnaire, this organizational method can help reduce employee stress. The use of stress monitoring software can enhance people's health as well as the welfare of society [11]. Thus, the development of scientific tools capable of analyzing physiological data and automatically estimating human stress levels is imperative. Health issues like obesity, heart attacks, diabetes, asthma, and other ailments can be brought on by stress. Every hour, a student in a different part of the nation ends their life [12]. A machine learning technique in artificial intelligence allows a system to learn and adapt without the need for explicit programming (AI). Making computer programs that can learn for themselves is known as "machine learning," a branch of computer science [13]. Digital signal processing, which considered the Galvanic skin response, blood volume, pupil dilation, and skin temperature, was used to assess earlier work on stress detection. Previous studies on this topic have used a range of physiological indicators and visual cues to quantify stress levels in focused individuals [14]. The following people have successfully completed the main contribution of the work:

- In this paper A novel STEP-YOLO has been proposed for detecting the Stress on IT Employees.
- Initially the input images are pre-processed in this pre-processing image acquisition and image processing are done to enhance the image.

- Then the features are extracted from the preprocessed image it extracts the feature whether they are happy, sad or neutral.
- Finally, the objects are detected using the YOLOv5 technique to detect the stress on IT employees.

The remaining portion of the research study was set up in this manner. In Section 2, the research is described using existing literature; In Section 3, the STEP-YOLO, a proposed approach for predicting coffee quality, is thoroughly explained; and in Section 4, the experiment's outcomes are discussed. Section 5 explains the outcome of the procedure and what comes next.

2. LITERATURE SURVEY

In 2020 Bobade, P. and Vani, M., [15] proposed a number of deep learning and machine learning techniques that employ multimodal datasets collected from physiological and wearable motion sensors to identify stress in individuals, which can shield a person from a variety of health issues caused by stress. The accuracy of the binary and three-class classifications were assessed and compared using machine learning techniques. With accuracy ratings of 84.32% and 95.21%, this model successfully completed the three-class and binary classification tasks.

In 2021 Sabour, R.M., et al [16] introduced a new dataset called UBFC-Phys that was gathered from subjects experiencing social stress both with and without contact. The objective of this is to exhibit the dataset, which makes available to the public, as well as the experimental findings of stress recognition and the comparison of contact and noncontact data. The application of remote PRV features resulted in an accuracy of 85.48 percent for stressed state detection.

In 2022 Mohan, L. and Panuganti, G., [17] focus on using the Perceived Stress Scale (PSS) for stress detection. The PSS approach is used because it is a simple questionnaire with proven psychometric features. The findings of this study, which employed the Random Forest, Logistic Regression, and SVM methodologies, indicate that only approximately 9.6% of workers are stress-free. The logistic regression approach yields the maximum prediction accuracy of 99 percent based on the experimental results.

In 2022 Giannakakis, G., et al [18] proposed a unique deep-learning pipeline to identify facial action units automatically. This focuses on identifying and analyzing automatic AUs as quantitative markers to differentiate between neutral and stressed states in videos. The suggested technique is used on the SRD'15 stress dataset, which has four different types of stressors associated with neutral and stressed states. Experimental detection of the stress-related AUs showed that, in contrast to neutral states, stress significantly increases their intensity, resulting in a more expressive human face.

In 2022 Yang, K., et al [19] Proposed a knowledge-aware mentalization module that considers the most pertinent knowledge aspects by utilizing dot-product attention. The research has potential applications for various mental health issues and makes it easier to identify and analyze stress and depression in social media data. This approach delivers new

state-of-the-art performance on all datasets, with an average improvement of 2.07%, as demonstrated by the experimental findings, with F1 scores of 95.4% on Depression Mixed, 83.5% on Dreaded, and 77.8% on SAD.

In 2023 Hamdi, E., et al [20] proposed a stress detection deep learning model trained and tested on the Stress Annotated Dataset (SAD). In the stress detection test, the model produces competitive results, suggesting that data augmentation greatly enhances performance. It is possible to investigate the impact on the stress detecting location by implementing various textual data augmentation processes that provide more data samples. The accuracy increases from 6.1% to 10.4% when different data augmentation strategies are implemented.

In 2023 Patel, A., et al [21] proposed a cutting-edge artificial intelligence (AI) technique based on deep learning (DL) that develops a model for the identification of emotional stress levels using electroencephalogram (EEG) data. The suggested method is verified using the publicly accessible Database for Emotion Analysis using Physiological Signals (DEAP), a benchmark dataset. The outcomes demonstrated that the CONVID+BiLSTM outperformed the traditional shallow learning techniques and offered the greatest emotion recognition accuracy of 88.03 % among the various built deep learning models.

3. PROPOSED METHOD

This method a novel STress DEtection on it employees using YOLO deep learning (STEP-YOLO) has been proposed for detecting the Stress on IT Employees. Initially, the input images are pre-processed in this pre-processing image acquisition and image processing are done to enhance the image. The features are extracted from the pre-processed image it extracts the feature whether they are happy, sad or neutral. Finally, the objects are detected using the YOLOv5 technique to detect the stress on IT employees.

3.1. Pre-Processing

Pre-processing images is an essential stage in computer vision and image analysis that highlights the best and most valuable images for subsequent tasks. A series of stringent methods for improving the caliber and value of images for future evaluation tasks are included.

3.1.1. Image Acquisition

Image acquisition for stress detection is the process of employing specialized imaging equipment to collect visual data that can reveal physiological or psychological stress signals. This usually consists of thermal cameras, highresolution cameras, or other sensors that may pick up on minute variations in skin tone, face expressions, or motions. In order to precisely capture the important elements, the method needs to guarantee ideal lighting and placement. As the foundation for further research utilizing algorithms intended to identify stress indicators, the quality and accuracy of the obtained images are vital. Reliable stress detection and assessment are made possible in this situation by effective image acquisition, which facilitates applications in user experience research, workplace monitoring, and healthcare. Block Diagram of the proposed STEP-YOLO method shown in Figure 1.

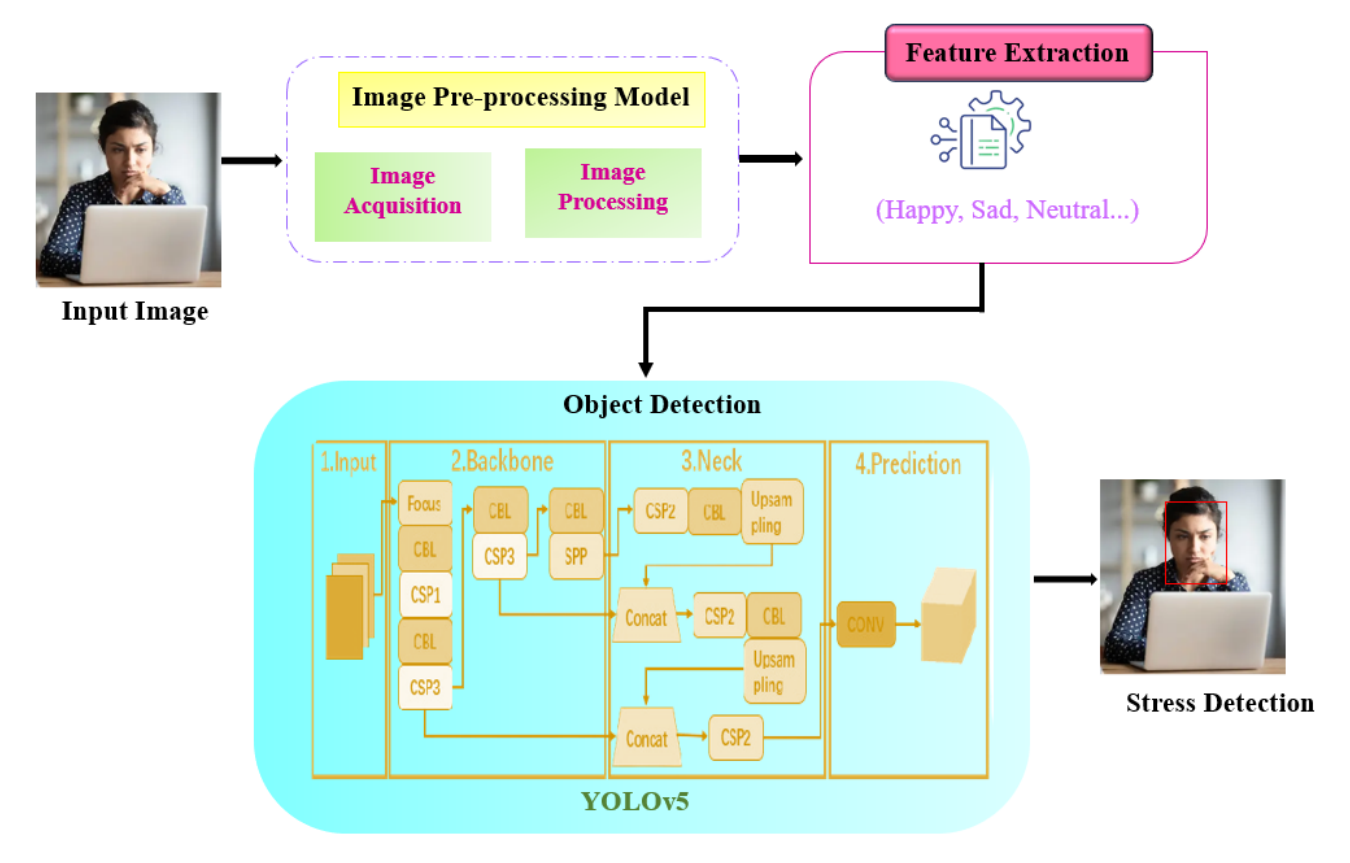


Figure 1. Block Diagram of the proposed STEP-YOLO method.

3.1.2. Image Processing

Analyzing images to find physiological or psychological signs of stress is known as image processing for stress detection. In order to identify important indicators like facial expressions, temperature variations on the skin, or microexpressions, this procedure involves pre-processing to improve image quality, such as noise reduction and contrast augmentation, followed by feature extraction algorithms. These features are interpreted and stress levels are quantified using sophisticated algorithms, such as machine learning models and pattern recognition. In order to enable applications in fields like mental health evaluation, human-computer interaction, and occupational health monitoring, the objective is to convert raw image data into insightful knowledge about an individual's stress level.

3.2. Feature Extraction

In order to detect stress in images feature extraction entails separating out and identifying particular visual cues that are correlated with stress levels. This procedure entails the identification and examination of characteristics such as variations in skin temperature, micro-expressions on the face, and other physiological indicators. The system can efficiently analyze and measure stress levels by concentrating on these stress-related characteristics, offering insightful information for applications in psychology, healthcare, and human-computer interaction.

3.3. Object Detection

The process of discovering and identifying things inside an image is known as object detection in images. The computer vision approach is categorized into predetermined groups using this method, which additionally draws bounding boxes around the items to indicate their exact locations.

3.3.1. YOLOv5

YOLOv5 was brought presented by Ultralytics, which advanced YOLOv4 largely on its foundation. It is a detection version that achieves a good balance between accuracy and speed by leveraging the advantages of earlier iterations and several networks, including CSPNet and PANet. This YOLO model family presents a scalable way to classify recyclables into several groups. Depending on the material, construction waste can be broadly divided into four classes: wood, stone, brick, and plastic taking into account. The YOLOv5 model has been selected because to its effectiveness and accuracy in identifying objects. The Head, Neck, and Backbone are the three main architectural blocks that make up this structure.

YOLOv5 Backbone

The basis of CSPDarknet is used for feature extraction from photos containing cross-stage partial networks. which is implemented by the YOLOv5 Backbone. By quickly down sampling the dataset's photos, the focus module may pass image information into the channel without causing any missing images is more thoroughly extracting the features of the image information. YOLOv5 model simplification, enhanced feature extraction from photos, and faster detection are all possible using the modules. The SPP module may efficiently increase the backbone features' receiving range, improve the dataset image's scale invariance, promote network convergence, and increase accuracy.

YOLOv5 Neck

YOLOv5 Neck aggregates the features building a feature pyramid network with PANet and sending it to the Head for prediction. YOLOv5's bottleneck layer mixes route aggregation network (PAN) and feature pyramid network (FPN) architectures. Images with deep features have less geographical information and more semantic information. Conversely, images with shallow features contain poorer semantic information and stronger location information. Semantic information can be transferred from the deep feature picture to the shallow feature image through FPN. PAN can be used to move location information from the deep feature layer to the shallow feature layer. FPN and PAN working together may aggregate parameters from several trunk levels and detection layers, significantly enhancing the network's capacity for feature fusion.

YOLOv5 Head

The layers in the head produce predictions based on the anchor boxes in order to detect objects. The two parts of the head are non-maximum suppression (NMS) and loss function. The location loss in YOLOv5 is calculated using the full Iou (CIoU) loss function, which additionally takes loss and confidence into consideration, whereas the binary cross entropy loss function is used to establish the categorization. The sum of all the losses is the total loss. By completely accounting for the overlap area, the distance from the center point, and the aspect ratio, the CIoU loss function accelerates and increases the accuracy of the prediction box's regression.

$$f_i = 2\tau(a_i) - 0.5 + e_i \tag{1}$$

$$f_i = 2\tau(a_i) - 0.5 + e_i \tag{2}$$

$$f_r = q_k (2\tau(a_r))^2 \tag{3}$$

$$f_v = q_v(2\tau(a_v))^2 \tag{4}$$

The upper left corner of the feature map has its coordinate value set to (0,0). The unadjusted coordinates of the anticipated Centre point are e_i and e_j . f_i , f_j , f_r and f_v stand for the updated prediction box's information. The information for the previous anchor is contained in q_k and q_v . The model's calculated offsets are denoted by the letters a_i and a_j the procedure of changing the final prediction box's center coordinate and size to match the center coordinate and size of the preset prior anchor.

4. RESULT AND DISCUSSION

This section discusses performance in terms of different assessment criteria and analyzes the experimental results of the proposed method. An i5 CPU and 4 GB of RAM were used to run the MATLAB simulator to assess the effectiveness of the proposed method.

4.1. Performance Evaluation

Evaluation measures were employed to verify the efficacy and characteristics of the proposed method. True Positive, False Positive, True Negative, and False Negative are the four basic metrics that are commonly used to assess performance. Employee facial detection is implemented through accuracy, Precision, Recall and F1-Score. The following expression was used to calculate the accuracy.

$$\begin{split} Accuracy &= \frac{\mathit{Tru}_{\mathit{Pos}} + \mathit{Tru}_{\mathit{Neg}}}{\mathit{Tru}_{\mathit{Pos}} + \mathit{Tru}_{\mathit{Neg}} + \mathit{Fal}_{\mathit{Pos}} + \mathit{Fal}_{\mathit{Neg}}} \times 100 \\ Precision &= \frac{\mathit{Tru}_{\mathit{Pos}}}{\mathit{Tru}_{\mathit{Pos}} + \mathit{Fal}_{\mathit{Pos}}} \\ Recall &= \frac{\mathit{Tru}_{\mathit{Pos}}}{\mathit{Tru}_{\mathit{Pos}} + \mathit{Fal}_{\mathit{Neg}}} \end{split}$$

Where Tru_{Pos} and Tru_{Neg} indicates the True Positive and True Negative of the input detection image. $Fa\ell_{Pos}$ and $Fa\ell_{Neg}$ indicates the False Positive and False Negative of the input image.

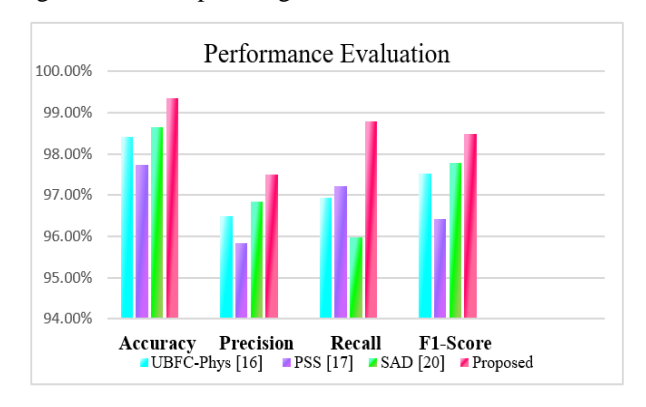


Figure 2. Performance Evaluation of the Proposed STEP-YOLO

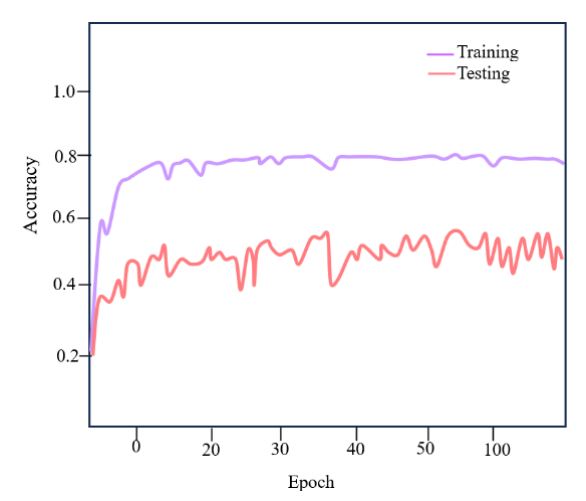


Figure 3. Accuracy Graph of the Proposed Method

Figure 2 describes the Performance evaluation of the proposed method with the existing methods such as UBFC-Phys, PSS and SAD. In this, the proposed method achieves an accuracy rate of 99.35%, a Recall rate of 98.79%, a Precision Rate of 97.51% and an F1-score of 98.48%. The proposed STEP-YOLO achieves an overall accuracy rate of 0.94%, 1.61% and 0.7% which is comparatively higher than the existing methods such as UBFC-Phys, PSS and SAD.

The accuracy and repetition of the proposed method are depicted in Figure 3. Plotting the Y-axis against the X-axis represents the overall quality of the epoch. The orange line here illustrates the testing period, and the violet line shows the training value of the proposal method.

Figure 4 describes the loss and iteration graph of the proposed method. Plotting the Y-axis against the X-axis represent the overall quality of the epoch.

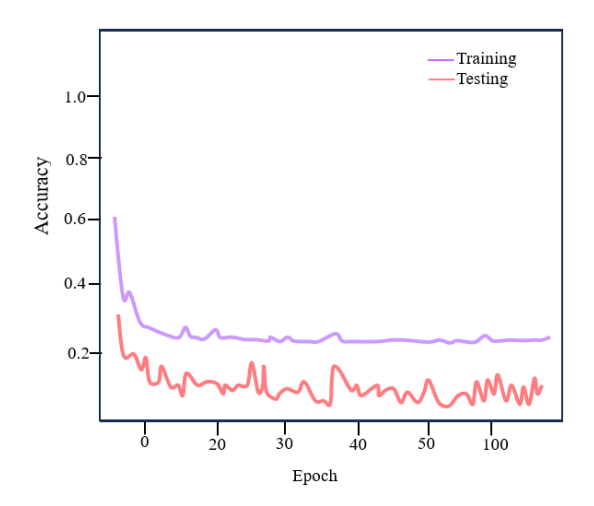


Figure 4. Loss Graph of the Proposed Method

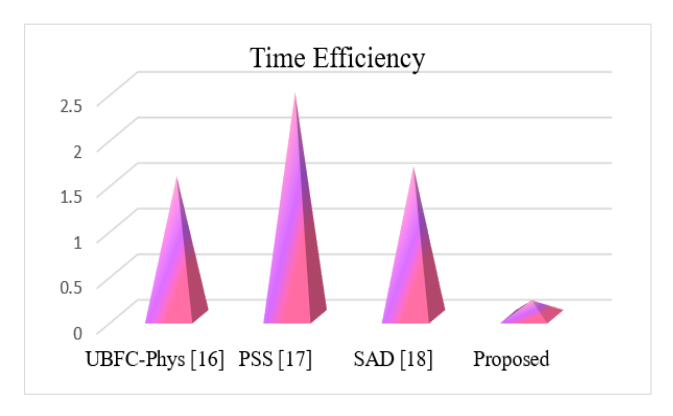


Figure 5. Time Efficiency of the Proposed STEP-YOLO

Figure 5 describes the time efficiency of the proposed and the Existing method such as UBFC-Phys, PSS and SAD. It shows that the proposed method takes 0.18 milliseconds which is comparatively less than the Existing method which takes 1.54, 2.46 and 1.65 milliseconds. This shows that the proposed method takes less time for detecting the stress in IT employees.

5. CONCLUSION

In this paper a novel Stress Detection on it employees using YOLO deep learning (STEP-YOLO) has been proposed for detecting the Stress on IT Employees. Initially, the input images are pre-processed in this pre-processing image acquisition and image processing are done to enhance the image. The features are extracted from the pre-processed image it extracts the feature whether they are happy, sad or neutral. Finally, the objects are detected using the YOLOv5 technique to detect the stress on IT employees. The proposed STEP-YOLO achieves an accuracy rate of 99.35% and an overall accuracy rate of 0.94%, 1.61% and 0.7% which is comparatively higher than the existing methods such as UBFC-Phys, PSS and SAD. The proposed method takes 0.18 milliseconds to detect the stress on IT employees which is comparatively less than the existing methods. The main added value of this article is that it helps the user to precisely recognize ongoing stress in order to decrease future health risk factors. The results are preliminary due to the small number of participants or technical details. Our plan to conduct more extensive demographic study in the future.

CONFLICTS OF INTEREST

The authors declare that they have no known competing financial interests or personal relationships that could have appeared to influence the work reported in this paper.

FUNDING STATEMENT

Not applicable.

ACKNOWLEDGEMENTS

The author would like to express his heartfelt gratitude to the supervisor for his guidance and unwavering support during this research for his guidance and support.

REFERENCES

- [1] Y.A. Hajam, R. Rani, S.Y. Ganie, T.A. Sheikh, D. Javaid, S.S. Qadri, S. Pramodh, A. Alsulimani, M.F. Alkhanani, S. Harakeh, and A. Hussain, "Oxidative stress in human pathology and aging: molecular mechanisms and perspectives", *Cells*, vol. 11, no. 3, pp. 552, 2022. [CrossRef] [Google Scholar] [Publisher Link]
- [2] D.B. O'Connor, J.F. Thayer and K. Vedhara, "Stress and health: A review of psychobiological processes", *Annual review of psychology*, vol. 72, pp. 663-688, 2021. [CrossRef] [Google Scholar] [Publisher Link]
- [3] C.T. Tran, H.T. Tran, H.T. Nguyen, D.N. Mach, H.S. Phan, and B.G. Mujtaba, "Stress management in the modern workplace and the role of human resource professionals", 2020. [CrossRef] [Google Scholar] [Publisher Link]
- [4] A. Carroll, L. Flynn, E.S. O'Connor, K. Forrest, J. Bower, S. Fynes-Clinton, A. York and M. Ziaei, "in their words: listening to teachers' perceptions about stress in the workplace and how to address it", Asia-Pacific Journal of Teacher Education, vol. 49, no. 4, pp. 420-434, 2021. [CrossRef] [Google Scholar] [Publisher Link]
- [5] D.L. Pandey, "Work stress and employee performance: an assessment of impact of work stress", *International Research Journal of Human Resource and Social Sciences*, vol.7, no. 05, pp. 124-135, 2020. [CrossRef] [Google Scholar] [Publisher Link]
- [6] O. Hämmig, "Work-and stress-related musculoskeletal and sleep disorders among health professionals: a cross-sectional study in a hospital setting in Switzerland", *BMC musculoskeletal disorders*, vol. 21, pp.1-11, 2020. [CrossRef] [Google Scholar] [Publisher Link]
- [7] J. Selimović, A. Pilav-Velić and L. Krndžija, "Digital workplace transformation in the financial service sector: Investigating the relationship between employees' expectations and intentions", *Technology in Society*, vol. 66, pp. 101640, 2021. [CrossRef] [Google Scholar] [Publisher Link]
- [8] S. Gedam and S. Paul, "A review on mental stress detection using wearable sensors and machine learning techniques", *IEEE Access*, vol. 9, pp. 84045-84066, 2021. [CrossRef] [Google Scholar] [Publisher Link]
- [9] R. Walambe, P. Nayak, A. Bhardwaj and K. Kotecha, "Employing multimodal machine learning for stress detection", *Journal of Healthcare Engineering*, pp.1-12, 2021. [CrossRef] [Google Scholar] [Publisher Link]
- [10] R.K. Nath, H. Thapliyal and A. Caban-Holt, "Machine learning based stress monitoring in older adults using wearable sensors and cortisol as stress biomarker", *Journal of Signal Processing Systems*, pp. 1-13, 2022. [CrossRef] [Google Scholar] [Publisher Link]
- [11] X. Han, L. Wang, S.H. Seo, J. He and T. Jung, "measuring perceived psychological stress in urban built environments using Google Street View and deep learning", *Frontiers in*

- *public health*, vol. 10, pp. 891736, 2022. [CrossRef] [Google Scholar] [Publisher Link]
- [12] M. Shehab, L. Abualigah, Q. Shambour, M.A. Abu-Hashem, M.K.Y. Shambour, A.I. Alsalibi and A.H. Gandomi, "Machine learning in medical applications: A review of state-of-the-art methods", *Computers in Biology and Medicine*, vol. 145, pp. 105458, 2022. [CrossRef] [Google Scholar] [Publisher Link]
- [13] S. Jayanthi, V. Priyadharshini, V. Kirithiga and S. Premalatha, "Mental health status monitoring for people with autism spectrum disorder using machine learning", *International Journal of Information Technology*, vol. 16, no. 1, pp. 43-51. 2024. [CrossRef] [Google Scholar] [Publisher Link]
- [14] O. Attallah, "An effective mental stress state detection and evaluation system using minimum number of frontal brain electrodes", *Diagnostics*, vol. 10, no. 5, pp. 292, 2020. [CrossRef] [Google Scholar] [Publisher Link]
- [15] P. Bobade and M. Vani, "Stress detection with machine learning and deep learning using multimodal physiological data", In 2020 Second International Conference on Inventive Research in Computing Applications (ICIRCA), pp. 51-57, IEEE. 2020, July. [CrossRef] [Google Scholar] [Publisher Link]
- [16] R.M. Sabour, Y. Benezeth, P. De Oliveira, J. Chappe and F. Yang, "Ubfc-phys: A multimodal database for psychophysiological studies of social stress", IEEE *Transactions on Affective Computing*, vol. 14, no. 1, pp. 622-636, 2021. [CrossRef] [Google Scholar] [Publisher Link]
- [17] L. Mohan and G. Panuganti, "Perceived Stress Prediction among Employees using Machine Learning techniques", *In 2022 International Conference on Communication, Computing and Internet of Things (IC3IoT), IEEE*, pp. 1-6. [CrossRef] [Google Scholar] [Publisher Link]
- [18] G. Giannakakis, M.R. Koujan, A. Roussos and K. Marias, "Automatic stress analysis from facial videos based on deep facial action unit recognition", *Pattern Analysis and Applications*, pp.1-15, 2022. [CrossRef] [Google Scholar] [Publisher Link]
- [19] K. Yang, T. Zhang and S. Ananiadou, "A mental state Knowledge–aware and Contrastive Network for early stress and depression detection on social media" *Information Processing & Management*, vol. 59, no. 4, pp. 102961, 2022. [CrossRef] [Google Scholar] [Publisher Link]

- [20] E. Hamdi, M. Mabrouk, S. Rady and M. Aref, "Data Augmentation Impact on Deep learning Performance for Stress Detection", In 2023 Eleventh International Conference on Intelligent Computing and Information Systems (ICICIS), pp. 160-165, 2023. [CrossRef] [Google Scholar] [Publisher Link]
- [21] A. Patel, D. Nariani and A. Rai, "Mental Stress Detection using EEG and Recurrent Deep Learning", In 2023 IEEE Applied Sensing Conference (APSCON), pp. 1-3. 2023, IEEE, [CrossRef] [Google Scholar] [Publisher Link]

AUTHORS



S. Abinisha was born in Kanyakumari district, Tamil Nadu, India in 2001. She received her BE degree in Computer Science and Engineering from Arunachala college of Engineering for women, Manavilai, Anna University, currently she is pursuing her ME degree in Computer Science and Engineering from Satyam College of Engineering and Technology, Aralvaimozhi, Anna University,

India. Her interested research area is Yolo deep learning algorithm-based IT employee stress.



S. S. Pooja received her B.E degree in CSE from Loyola Institute of Technology & Science, Anna University, in 2020 and obtained M.E degree in CSE from Loyola Institute of Technology & Science in 2023

Arrived: 20.05.2024 Accepted: 10. 06.2024



RESEARCH ARTILE

DEEP LEARNING MODEL FOR ACCURATE BRAIN TUMOR DETECTION USING CT AND MRI IMAGING

R. Abirami 1,* and P. Krishna Kumar 2

¹ Department of Computer Science and Engineering, Amrita college of engineering and Technology, Nagercoil, India.

² Department of Computer Science and Engineering, Amrita Vishwa Vidyapeetham, Nagercoil, India.

*Corresponding e-mail: abiramisep14@gmail.com

Abstract - Brain tumors (BT) are a very common, deadly condition with a very poor prognosis at the most aggressive grade. BT represent a prevalent and fatal condition with particularly poor prognosis at advanced stages. Accurate diagnosis and classification are critical for effective treatment planning and patient care. This study introduces a novel deep learning-based algorithm for early BT detection using CT and MRI images. The proposed model enhances image quality using Adaptive Trilateral filtering, extracts feature via the MobileNet model, selects relevant features through the Tyrannosaurus optimization algorithm, and classifies brain tumors with a Deep Belief Network (DBN). The model categorizes tumors into three classes: pituitary tumor, no tumor, and glioma tumor. In comparison to conventional deep learning networks, the model performs better in experiments using the BRATS2020 dataset, reaching a 99.3% accuracy rate and great dependability. This paper offers significant improvements in automated brain tumor detection, promising better patient outcomes through early and precise diagnosis.

Keywords – Brain Tumor, Deep Learning, Deep Belief Network, Mobile Net.

1. INTRODUCTION

ISSN: xxxx-xxxx

Worldwide, the frequency of brain tumors is rising quickly, and millions of people die from them every year [1]. For brain cancers to be effectively treated, proper diagnosis and categorization are crucial. Appropriate patient care and the development of a effective treatment plan depend on a timely diagnosis [2]. In order to manually classify brain tumor MR images with comparable structures or features, radiologists must be capable of reliably identifying and classifying brain cancers. In addition to acting as the administrative hub, the human brain is a vital component of the nervous system that handles daily activities [3,4]. The human body's sensory organs send impulses or signals to the brain, which then receives, interprets, and makes a decision about them before sending the data to the muscles [5]. One of the most serious conditions affecting the human brain, BTs, is characterized by abnormal brain cell development that is irregular [6,7]. There are two main kinds of BT: primary and secondary metastatic.

Brain tumors can be identified and their progression monitored during the diagnosis and therapy phases using brain MRI and CT scans [8]. Automated medical image analysis is heavily influenced by the high-resolution images obtained from MRIs and CT scans, which provide extensive insights into brain disorders and structure [9,10]. Brain tumor classification, data analysis, and professional diagnosis are the main uses of image processing and deep learning algorithms [11,12]. Deep neural networks have made it possible to segment brain tumors successfully thanks to recent developments in medical imaging [13]. This article proposes a deep learning-based algorithm for early BT detection using CT and MRI images. The main contribution of the proposed model is organized as follows.

- Initially, the input images are pre-processed utilizing Adaptive Trilateral filter to expand the quality of the image.
- Then, Mobile Net model is employed for extracting the features in the pre-processed brain image.
- The extracted image features are selected using Tyrannosaurus optimization Algorithm.
- Afterward, the selected features are fed into the DBN model to classify the Three cases of brain tumour.

The remaining sections of the research paper adhere to the following structure: Chapter 2 provides detailed summaries of relevant works, while Chapter 3 offers a comprehensive explanation of the proposed model for early recognition of brain tumors. Chapter 4 encompasses the experimental outcomes and discussion, and lastly, Chapter 5 contains the conclusion and outlines future work.

2. LITERATURE SURVEY

In 2022, Ottom, M.A., et al., [14] developed a Dl model for 2D BT subdivision in MR images and conveying the intrinsic commonalities of a more narrowly defined collection of tumors via Znet and deep neural networks (DNN). The experiment's accuracy rate was 99.6%. The

disadvantages of Znet include that it requires a large number of annotated ground truths (labels), which adds time to the process and necessitates rigorous testing.

In 2022, Gaur, et al., [15] introduced an explanation-driven DL model for the use of an MRI image collection in the prediction of different types of brain cancer utilizing CNN, LIME, and Shapley additive explanation (SHAP). Even if the model in use has an accuracy of 94.64%, the reliability rate is still insufficient for the classification.

In 2022, Haq, et al., [16] developed a hybrid, thorough method that uses CNN to accurately classify brain MRI cancers. The intended CNN and SVM-RBF classifier yielded a 98.30% reliability rate. The recommended model has noticeably superior performance than state-of-the-art methods, as exposed by the segmentation and classification results. The time-consuming aspect of this strategy is a disadvantage.

In 2023, Mostafa, et al., [17] suggested an automatic technique to categorize brain cancers using MRI pictures. The BT segmentation dataset, which was developed as a standard for emerging and accessing systems for BT division and analysis, includes the suggested MRI pictures of BTs. Image feature extraction using DCNN with a U-Net model is used to accomplish this aim. Through training on the BraTS dataset, a 98% overall accuracy model was created.

In 2024, Geetha, et al., [18] presented a new SCAOA to categorize the brain tumor. It extracts the aspects involving statistics and texturing. The Archimedes Optimization Algorithm (AOA) and the Sine Cosine Algorithm (SCA) are combined to create the suggested SCAOA. Even though the suggested SCAOA-based Dense Net achieves the maximum

accuracy of 93%, the dependability rate is insufficient for BT detection.

In 2024, Sharif, et al., [19] recommended that an end-toend optimized DL system be used to construct a multimodal brain tumor classification system. A CNN model is trained and the contrast along the ant colony optimization strategy is improved using hybrid division histogram equalization. An MC-SVM receives the fused result after it has been combined using a matrix length technique. In the research investigation, the suggested method had a 99.06% accuracy rate.

In 2024, Akter, et al., [20] suggested a deep CNN-based architecture and a U-Net-based segmentation model for the automatic classification of brain pictures into four classifications. Two classification techniques are also assessed according to AUC, accuracy, recall, and precision. The top correctness of 98.7% was attained by the classification model with the assistance of the segmentation approach, according to the results.

3. PROPOSED METHOD

In this section, a novel deep learning-based method has been proposed for early BT recognition from CT and MRI images. To progress the image quality, the input images are first pre-processed using an Adaptive Trilateral filter. The features in the previously processed brain image are then extracted using the Mobile Net model. Tyrannosaurus optimization algorithm is used to choose the features from the retrieved image. The three brain tumor cases are then classified using the features that were chosen and supplied into the Deep Belief Network model. Figure 1 shows the proposed architecture.

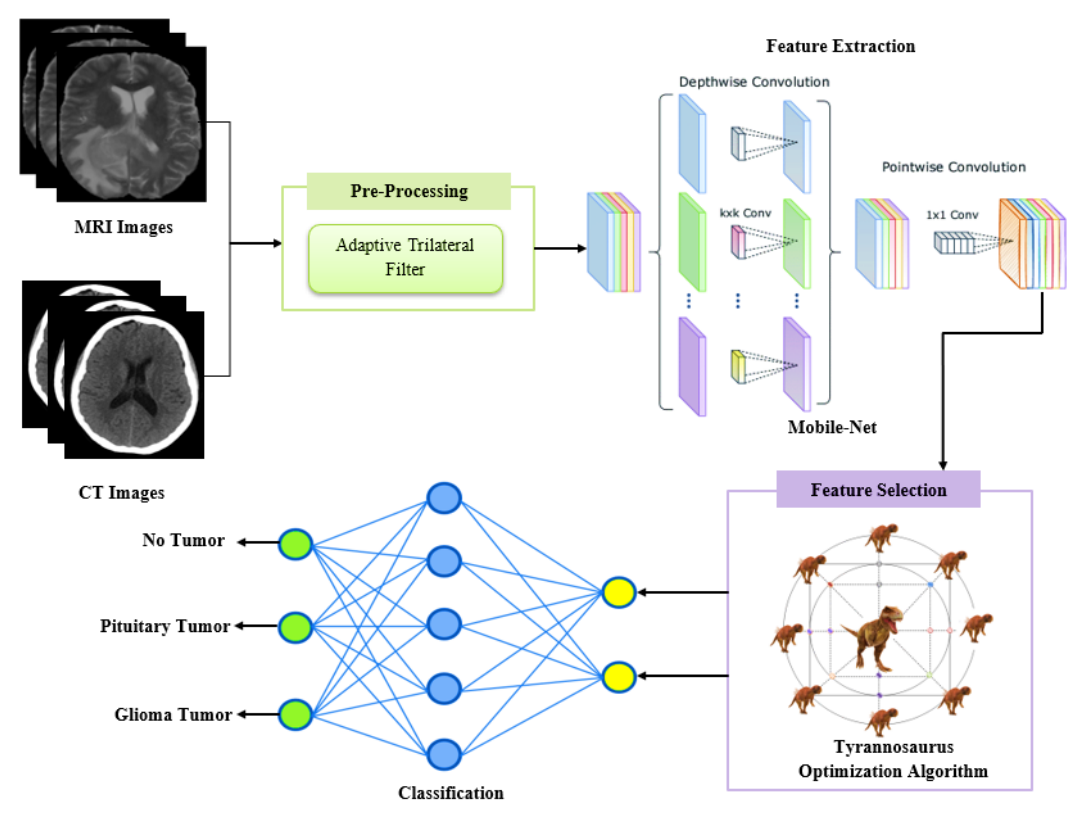


Figure 1. Architecture of Proposed Methodology

3.1. Image Pre-Processing

Image preprocessing is a perilous step in tumour detection, as it makes raw image data for more analysis and processing. The input images are under go pre-processing via the AT filter method to enhance the images.

3.1.1. Adaptive Trilateral Filter

AT filter is used in pre-processing to eliminate noise artefacts from the input medical images. It implements the guiding principles of the bilateral filter. The tilting angle ti_{\emptyset} of a trilateral filter is produced when a bilateral filter is applied to the picture data. This is because, given ti_{\emptyset} at the target pixel, a should average highly related surrounding pixels and exclude dissimilar pixels.

$$ti_{\emptyset}(x) = \frac{1}{k_{\emptyset}} \sum_{x} \sum_{a} f_{a} c(x, a) b(f_{x}, f_{a})$$
 (1)

When the kernel is tilted, the trilateral filter's c (.) and b (.) functions become non-orthogonal. Eqn (2) gives the value of each pixel at this plane.

$$g(x,a) = f(x) + ti_{\emptyset}.(||x-a||)$$
 (2)

where x at a target pixel represents f(x), the intensity, and ||x - a|| is the dimensional separation between x and a. The tilting angle is denoted by ti_{\emptyset} . To find the output of a trilateral filter, the resulting image is first passed through a bilateral filter, and then the value g is removed from the surrounding area of the target pixel.

$$f_{op}(x) = f_{ip}(y) + L(y)\rho \tag{3}$$

where ρ is the spatial distance between pixels x and a, and $f_{op}(x)$ is the output function. Tilting improves the filter's capacity to smooth high gradient zones.

3.2. Feature Extraction

Feature extraction in brain tumor detection involves identifying and isolating specific characteristics from medical images, such as MRI scans and CT scans, The preprocessed image undergoes feature extraction using MobileNet.

3.2.1. Mobile Net

MobileNet is a deep learning architecture well-suited for feature extraction in image recognition tasks. It utilizes a series of convolutional layers to progressively extract features from images. Standard convolutional layers in the initial stages capture basic features like edges and corners. The following depthwise separable convolutions are efficient at extracting spatial information from the image. Batch normalization and ReLU activation layers maintain stability and introduce non-linearity for improved learning. Emphasize the global average pooling layer as the key step for feature extraction.

The function of the dimension multiplier δ is to compress the connection equally at each tier. The dimension multiplier is applied to lower the width α of the source image. Equation (4) describes the total value of the C_s computations for the network's central layers.

$$C_s = E_c. E_c. \delta J_{p.} \alpha E_{n.} \alpha E_{n.} + \delta J_{p.} \delta J_{o.} \alpha E_{n.} \alpha E_n$$
 (4)

Since the characteristic map is represented by $E_n \times E_n$ in equation (4) above, the kernel dimension is $E_c \times E_c$, the source data channel is J_p , and the output data is J_o . For the purpose of identifying illnesses in tea leaves, the width factor $\alpha = 1$ and the depth factor $\delta = 1$ were expressed. Equation (5) yields the typical convolution's computing cost O_o .

$$O_o = E_c.E_c.J_pJ_o.E_n.E_n (5)$$

Finally, the traditional resolution into depth-wise convolutional and point-wise convolution is used to estimate the reduction R_d for the feature extraction, that is stated in equation (6).

$$R_b = \frac{\alpha \cdot \mu^2}{I_0} + \frac{\alpha^2 \cdot \mu^2}{E^2 c} \tag{6}$$

By utilizing the above equations Mobile Net model successfully extract the features of pre-processed MRI and CT scan images.

3.3. Feature Selection

Feature selection involves choosing the most relevant features from extracted images to improve model performance and reduce computational burden. It enhances accuracy by focusing on discriminative attributes, filtering out noise, and diminishing overfitting.

3.3.1. Tyrannosaurus optimization Algorithm (T-Rex)

The T-Rex optimization approach is proposed for selecting the features from extracted features of MRI scan and CT scan images. The T-Rex is introduced based on the social behavior of Tyrannosaurus. The prey-predictor hunting method is the source of inspiration for this tactic. In addition to this technique, the position of the prey and the T-Rex are generated at random. The hunting is done based on where the prey is nearest. The Tyrannosaurus Rex pursues its prey until it seizes them; in the interim, the victim makes an effort to escape the T-Rex.

3.3.1.1. Initialization

The number of preys in a search area is randomly generated by the population-based TROA algorithm. Tyrannosaurus here refers to the task, and prey is the server's processing power. As shown in equation (7), y_n refer to the prey region or processing, which is randomly created within higher and lower bounds in a search area.

$$y_n = r(j_c, i_c) * (v_f - u_g) + u_g$$
 (7)

Where n=1,2...m, m is the measurement, j_c is the number of populations, i_c is the measurement of the hunt space, v_f is the top restrict and u_g is the decrease restrict, and $y_n=[y_1,y_2,...y_m]$ is the prey area. When the estimate of reaching the dispersed prey is represented by the F_c .

$$Y_m = \begin{cases} X_m & \text{if } r() < F_c \\ Random & \text{else} \end{cases}$$
 (8)

3.3.1.2. Selection

The Selection relies upon at the area of prey, i.e. area of the server prey and the hunting area. If the hunter fails to hunt then, the prey area will become 0. It is found out through evaluating the fitness function.

$$X_l^{m+1} =$$
{update the target position if $f(X) < f(X_m)$ }
target is none otherwise

Where, f(X) is the fitness function for the prey position, and $f(X_m)$ is the fitness function for updated prey position.

3.4. Classification

DBN is a type of deep learning model consisting of multiple layers of Restricted Boltzmann Machines (RBMs), stacked hierarchically. The number of layers in DBNs correlates with the complexity of input data, while the number of output layers corresponds to the range of categories. DBNs use hidden variables to model data distributions. A two-step learning approach is employed: firstly, RBMs are trained greedily layer by layer to capture basic data patterns, then the entire system is fine-tuned to minimize the gap between original and reconstructed data. This process demands significant computational resources and persistence, but yields valuable results. The main characteristic of a DBN, h is determined by an RBM and learns $t\left(\frac{o}{p}, h\right)$. The previous average, $p\left(\frac{k}{h}\right)$, for concealed carriers. Equation (9) expresses the pace at which an apparent gradient is produced. Equation (10) represents the hidden layer of the DBN, with $sum(t_i)$ indicating the applied vector in the layer.

$$T(o) = \sum_{k} \left(p \, \frac{k}{h} t \left(\frac{o}{n}, h \right) \right) \tag{9}$$

$$sum(t_j) = \sum_{q_u=1}^{j} M(pjg_u)$$
 (10)

The output of the hidden or invisible layer based on the weight and bias of the images be depicted in equation (21).

$$E^{j} = \left[\sum_{i=1}^{k} \mathfrak{x}_{iL}^{F^{r}} * \mathfrak{Z}_{i}\right] E_{i} \,\forall \mathfrak{f}_{i} = w_{i}^{2} \tag{11}$$

 E^{j} represents the hidden layer bias of data and E_{j} be the output of the RBM layer for the multilayered classification process. The most representative features for modeling the data are those obtained in the layer of the DBN is expressed in equation (12).

$$Q_h = q_{t1}, q_{t2}, \dots, q_{ti} \tag{12}$$

Where t stands for the network's top layer, i for the number of features in multilayer networks, and Q_h for the DBN input vector. Finally, the brain tumors are classified as no tumor, pituitary tumor, and glioma tumor.

4. RESULTS AND DISCUSSION

This subsection uses the BRATS2020 dataset to evaluate the effectiveness of the suggested model. The source of the input MRI images is the BRATS2020 dataset.

The visualization outcomes of the proposed approach utilizing the BRATS2020 dataset are shown in Figure 2(a & b). Denoising the input CT and MRI images of brain tumors (column:1) improves picture quality and eliminates distortions (column:2). These previously processed photos are fed into Mobile Net concurrently in order to extract the features (column:3). Subsequently, patients' various brain tumor cases are distinguished using the categorization strategy (column:4).

Input	Pre-Processing	Feature Extraction	Result
		0	Normal
			Pituitary Tumor
			Glioma Tumor

Figure 2 (a). Experimental Results of the Brain CT images of Proposed Model

Input	Pre-Processing	Feature Extraction	Result
			Normal
A	A		Pituitary Tumor
			Glioma Tumor

Figure 2 (b). Experimental Results of the Brain MRI images of Proposed Model

4.1. Performance Analysis

The evaluation metrics previously described can be generated with simple parameters such as True Positive (t p_{os}), True Negative (t N_{eg}), False Positive (F p_{os}), and False Negative (FN_{eg}).

$$Acc = \frac{t p_{os} + t N_{eg}}{t p_{os} + t N_{eg} + F p_{os} + F N_{eg}} \times 100$$
(13)

$$Pre = \frac{t p_{0s}}{t p_{os} + F p_{os}} \tag{14}$$

$$Recall = \frac{t \, p_{\text{os}}}{t \, p_{\text{os}} + F N_{eg}} \tag{15}$$

$$F1.S = \frac{2}{\frac{1}{(Recall)} + \frac{1}{(Pre)}} \tag{16}$$

The efficiency of the planned model by classifying Brain Tumor, is shown in the Table.1. The proposed model has a 99.3% accuracy rate. Additionally, the proposed Attention Link Net achieves an F1 score of 98.09%, respectively.

Table 1. Evaluation of results of the proposed Model

Classes	Accuracy	Precision	Recall	Specificity	F1 score
Glioma tumor	99.42	98.02	98.27	98.04	98.46
Pituitary tumor	99.35	98.66	96.75	95.97	98.39
No tumor	99.13	95.45	97.15	96.64	97.44

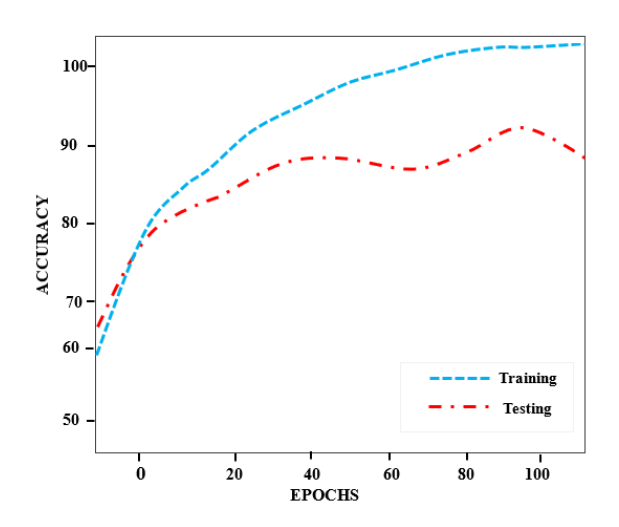


Figure 3. Accuracy of proposed model

The accuracy graph in Figure 3 was produced with a reliability range and 100 epochs. As the number of epochs increases, the proposed DBN's success rate also improves.

Figure 4 illustrates the relationship between epochs and loss, indicating a decrease in loss as the number of epochs increases. Utilizing MRI images and CT images, the proposed model exhibits a high level of reliability in identifying different stages of Brain Tumor. The detection

accuracy of the DBN model with 100 training epochs was 99.3, and it had a low rate of errors.

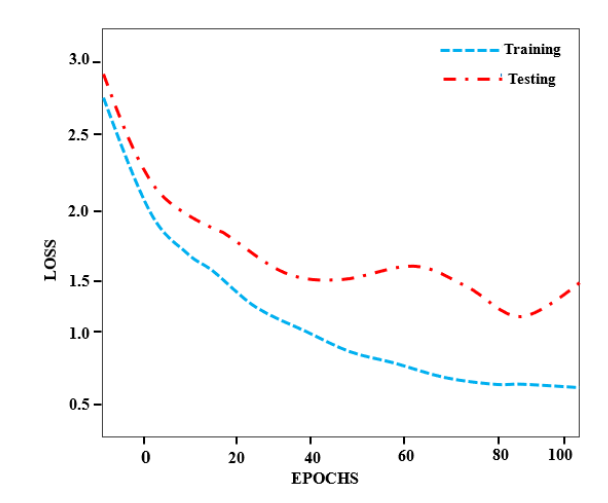


Figure 4. Loss of proposed Model

4.2. Comparative analysis

The efficiency of each neural network was assessed to confirm that the suggested model produces results with an outstanding level of reliability. The proposed model is compared with three deep learning classifiers Link Net, Reg Net, Res Net.

Table 2. Comparison of different approaches

NETWORKS	Accuracy	Precision	Recall	Specificity	F1 score
Link Net	98.05	96.31	96.42	95.24	96.04
Reg Net	97.09	96.76	97.30	96.13	96.39
Res Net	99.07	97.22	97.30	96.11	95.72
Proposed Model	99.3	97.37	97.39	96.88	98.03

The accuracy attained by the proposed model is 99.3%, which is higher than the traditional DL networks. The proposed model has high accuracy than Link Net, Reg Net, and Res Net which obtains 1.25%, 2.21%, and 0.23% while having a significantly lower computational cost than other networks.

Table 3. Compare the performance of existing models and the proposed model

AUTHOR	METHODS	ACCURACY
Haq, et al [16]	SVM-RBF	98.30%
Mostafa, et al., [17]	DCNN	98%
Sharif, et al., [19]	MC-SVM	99.06%
Proposed model	DBN	99.3%

According to the comparison Table above, the suggested model outperforms the SVM-RBF, DCNN, and MC-SVM in terms of overall accuracy by 1%, 1.3%, and 0.24%, respectively. The suggested network, however, outperformed the earlier networks in terms of performance. Because of this, the results of the suggested model for classifying cases of brain tumors are quite trustworthy.

CONFLICTS OF INTEREST

This paper has no conflict of interest for publishing.

FUNDING STATEMENT

Not applicable.

ACKNOWLEDGEMENTS

The author would like to express his heartfelt gratitude to the supervisor for his guidance and unwavering support during this research for his guidance and support.

REFERENCES

- [1] J.G. Gurney, and N. Kadan-Lottick, "Brain and other central nervous system tumors: rates, trends, and epidemiology", *Current opinion in oncology*, vol. 13, no. 3, pp. 160-166, 2001. [CrossRef] [Google Scholar] [Publisher Link]
- [2] R. Ahmed, M.J. Oborski, M. Hwang, F.S. Lieberman, and J.M. Mountz, "Malignant gliomas: current perspectives in diagnosis, treatment, and early response assessment using advanced quantitative imaging methods", Cancer management and research, pp. 149-170, 2014. [CrossRef] [Google Scholar] [Publisher Link]
- [3] A. May, "Experience-dependent structural plasticity in the adult human brain", *Trends in cognitive sciences*, vol. 15, no. 10, pp. 475-482, 2011. [CrossRef] [Google Scholar] [Publisher Link]
- [4] A. Iriki, and M. Taoka, "Triadic (ecological, neural, cognitive) niche construction: a scenario of human brain evolution extrapolating tool use and language from the control of reaching actions", *Philosophical Transactions of the Royal Society B: Biological Sciences*, vol. 367, no. 1585, pp.10-23, 2012. [CrossRef] [Google Scholar] [Publisher Link]
- [5] U. Proske, and S.C. Gandevia, "The proprioceptive senses: their roles in signaling body shape, body position and movement, and muscle force", *Physiological reviews*, 2012. [CrossRef] [Google Scholar] [Publisher Link]
- [6] N.A. Siddiqui, T. Qadri, M. Tayyab, U. Shahid, and S. Raza, "Recent Segmentation Trends of MRI-Based Brain Neoplasm: A Review", *Journal of Applied Engineering & Technology* (*JAET*), 7(1), pp.57-92, 2023. [CrossRef] [Google Scholar] [Publisher Link]
- [7] M. Ahmed Hamza, H. Abdullah Mengash, S.S. Alotaibi, S.B.H. Hassine, A. Yafoz, F. Althukair, M. Othman, and R. Marzouk, "Optimal and efficient deep learning model for brain tumor magnetic resonance imaging classification and analysis", *Applied Sciences*, vol. 12, no. 15, pp.7953, 2022. [CrossRef] [Google Scholar] [Publisher Link]
- [8] M.A. Weber, F.L. Giesel, and B. Stieltjes, "MRI for identification of progression in brain tumors: from morphology to function", Expert Review of Neurotherapeutics, vol. 8, no. 10, pp.1507-1525, 2008. [CrossRef] [Google Scholar] [Publisher Link]
- [9] E.D. Bigler, "Structural image analysis of the brain in neuropsychology using magnetic resonance imaging (MRI) techniques", *Neuropsychology Review*, vol. 25, pp. 224-249, 2015. [CrossRef] [Google Scholar] [Publisher Link]
- [10] F. Altaf, S.M. Islam, N. Akhtar, and N.K. Janjua, "Going deep in medical image analysis: concepts, methods, challenges, and future directions", *IEEE Access*, vol. 7, pp. 99540-99572, 2019. [CrossRef] [Google Scholar] [Publisher Link]
- [11] K. Muhammad, S. Khan, J. Del Ser, and V.H.C. De Albuquerque, "Deep learning for multigrade brain tumor classification in smart healthcare systems: A prospective survey", *IEEE Transactions on Neural Networks and Learning Systems*, vol. 32, no. 2, pp. 507-522, 2020. [CrossRef] [Google Scholar] [Publisher Link]
- [12] P. Gao, W. Shan, Y. Guo, Y. Wang, R. Sun, J. Cai, H. Li, W.S. Chan, P. Liu, L. Yi, and S. Zhang, "Development and validation of a deep learning model for brain tumor diagnosis and classification using magnetic resonance imaging", *JAMA Network Open*, vol. 5, no. 8, pp. e2225608-e2225608, 2022.
 [CrossRef] [Google Scholar] [Publisher Link]
- [13] M. Havaei, A. Davy, D. Warde-Farley, A. Biard, A. Courville, Y. Bengio, C. Pal, P.M. Jodoin, and H. Larochelle, "Brain tumor segmentation with deep neural networks", *Medical image analysis*, vol. 35, pp.18-31, 2017. [CrossRef] [Google Scholar] [Publisher Link]

- [14] M.A. Ottom, H.A. Rahman, and I.D. Dinov, "Znet: deep learning approach for 2D MRI brain tumor segmentation", IEEE Journal of Translational Engineering in Health and Medicine, vol. 10, pp.1-8, 2022. [CrossRef] [Google Scholar] [Publisher Link]
- [15] L. Gaur, M. Bhandari, T. Razdan, S. Mallik, and Z. Zhao, "Explanation-driven deep learning model for prediction of brain tumour status using MRI image data", Frontiers in genetics, vol. 13, pp.448, 2022. [CrossRef] [Google Scholar] [Publisher Link]
- [16] E.U. Haq, H. Jianjun, X. Huarong, K. Li, and L. Weng, "A hybrid approach based on deep cnn and machine learning classifiers for the tumor segmentation and classification in brain MRI", Computational and Mathematical Methods in Medicine, vol. 2022, 2022. [CrossRef] [Google Scholar] [Publisher Link]
- [17] A.M. Mostafa, M. Zakariah, and E.A. Aldakheel, "Brain Tumor Segmentation Using Deep Learning on MRI Images", *Diagnostics*, vol. 13, no. 9, pp. 1562, 2023. [CrossRef] [Google Scholar] [Publisher Link]
- [18] M. Geetha, V. Srinadh, J. Janet, and S. Sumathi, "Hybrid archimedes sine cosine optimization enabled deep learning for multilevel brain tumor classification using mri images", *Biomedical Signal Processing and Control*, vol. 87, pp.105419, 2024. [CrossRef] [Google Scholar] [Publisher Link]
- [19] M.I. Sharif, J.P. Li, M.A. Khan, S. Kadry, and U. Tariq, "M3BTCNet: multi model brain tumor classification using metaheuristic deep neural network features optimization", *Neural Computing and Applications*, vol. 36, no. 1, pp.95-110, 2024. [CrossRef] [Google Scholar] [Publisher Link]
- [20] A. Akter, N. Nosheen, S. Ahmed, M. Hossain, M.A. Yousuf, M.A.A. Almoyad, K.F. Hasan, and M.A. Moni, "Robust clinical applicable CNN and U-Net based algorithm for MRI classification and segmentation for brain tumor", *Expert Systems with Applications*, vol. 238, pp.122347, 2024. [CrossRef] [Google Scholar] [Publisher Link]

AUTHORS



R. Abirami was born in virudhunagar district, Tamil Nadu, India in 1996.she received her BE degree in computer science and Engineering from DMI Engineering college, Aralvaimozhi, Anna University, currently she is pursuing her ME degree in computer science and Engineering from Amrita college of engineering and technology, Nagercoil, Anna University, India. Her intrested research area is deep learning, Image processing

and Artificial intelligence.



P. Krishna Kumar received the B.E. Degree in Computer Science and Engineering from Bharathidasan University, India in 1992, received M.E. Degree in Computer Science and Engineering from Anna University, India in 2007 and Ph.D. degree in Information and Communication Engineering from Anna University, India in 2017.He has more than 9

years of industrial experience in the field of Software and 21 years of teaching experience. Presently he is working in Amrita Vishwa Vidyapeetham, Nagercoil Campus. His area of interest includes Network Security, Datamining, Cloud computing, Medical Image Processing, Deep Learning and Big data analysis. He has more than 20 International Journal Publication in his credit.

Arrived: 25.05.2024 Accepted: 16.06.2024